Journal of Medicinal Chemistry

Article

The discovery, SAR and biological characterization of a novel series of 6-((1H-pyrazolo[4,3-b]pyridin-3-yl)amino)-benzo[d]isothiazole-3-carboxamides as positive allosteric modulators of the metabotropic glutamate receptor 4 (mGlu4)

Sean Bollinger, Darren W. Engers, Joseph D. Panarese, Mary West, Julie L Engers, Matthew T. Loch, Alice L Rodriguez, Anna L. Blobaum, Carrie K. Jones, Analisa Thompson Gray, P. Jeffrey Conn, Craig W Lindsley, Colleen M Niswender, and Corey R. Hopkins

J. Med. Chem., **Just Accepted Manuscript** • DOI: 10.1021/acs.jmedchem.8b00994 • Publication Date (Web): 24 Sep 2018

ACS Publications

is published by the American Chemical Society. 1155 Sixteenth Street N.W., Washington, DC 20036

The discovery, SAR and biological characterization of a novel series of 6-((1*H*-pyrazolo[4,3-*b*]pyridin-3-yl)amino)-benzo[*d*]isothiazole-3-carboxamides as positive allosteric modulators of the metabotropic glutamate receptor 4 ($mGlu_4$)

Sean R. Bollinger[a,b], Darren W. Engers[a,b], Joseph D. Panarese[a,b], Mary West[a,b], Julie L. Engers[a,b], Matthew T. Loch[a,b], Alice L. Rodriguez[a,b], Anna L. Blobaum[a,b], Carrie K. Jones[a,b], Analisa Thompson Gray[a,b], P. Jeffrey Conn[a,b,c], Craig W. Lindsley[a,b,d,e], Colleen M. Niswender[a,b,c], Corey R. Hopkins[a,b,d,*]

[a]Vanderbilt Center for Neuroscience Drug Discovery, Vanderbilt University, Nashville, TN 37232, USA
[b]Department of Pharmacology, Vanderbilt University, Nashville, TN 37232, USA
[c]Vanderbilt Kennedy Center, Vanderbilt University Medical Center, Nashville, TN 37232, USA
[d]Department of Chemistry, Vanderbilt University, Nashville, TN 37232, USA
[e]Department of Biochemistry, Vanderbilt University, Nashville, TN 37232, USA

Abstract:

This work describes the discovery and characterization of novel 6-((1*H*-pyrazolo[4,3-*b*]pyridin-3-yl)amino-benzo[*d*]isothiazolole-3-carboxamides as $mGlu_4$ PAMs. This scaffold provides improved metabolic clearance and CYP1A2 profiles compared to previously discovered $mGlu_4$ PAMs. From this work, **27o** (VU6001376) was identified as a potent (EC_{50} = 28 nM, 49% Glu Max) and selective $mGlu_4$ PAM with an excellent rat DMPK profile (*in vivo* rat CL_p = 3.1 mL/min/kg, $t_{1/2}$ = 445 min, CYP1A2 IC_{50} > 30 μM). **27o** was also active in reversing haloperidol induced catalepsy in a rodent preclinical model of Parkinson's disease.

INTRODUCTION

Parkinson's disease (PD), first described 200 years ago, is the second most common neurodegenerative disease (Alzheimer's disease) and affects >10 million adults, globally.[1] The estimated economic burden of PD is estimated at $25 billion per year in the US alone.[2] The

prevalence increases with age and PD affects ~1% of the population above the age of 60.[3] PD is a movement disorder that is due to the loss of dopaminergic neurons in the substantia nigra pars compacta (SNpc) – expressing as a reduction in voluntary movement. The hallmark signs of PD include tremor at rest, bradykinesia, rigidity and disturbance of posture; these signs have not changed since the disease was first established in 1817.[4] The cause of PD is unknown, with a genetic factor being identified in a small portion of patients and environmental factors being associated with an increased risk of PD.[1, 3] Unfortunately, there are no disease-modifying treatments for PD, with only palliative treatments with dopamine replacement strategies (L-DOPA) as the main options.[5-7] Although L-DOPA does provide significant improvement in symptoms early in the treatment protocol, there are multiple side effects associated with long-term treatment.[5-8]

Within the basal ganglia (BG), connections are arranged as a set of direct and indirect pathways which act in a proper balance in a normal functioning BG.[9-11] However, an upset of this balance of the direct and indirect pathways results in motor dysfunctions, with a stronger signal coming from the indirect pathway (inhibiting and/or slowing movement).[11] Thus, multiple receptor classes that are present along the indirect pathway have been studied in order to identify novel targets that may provide disease-modifying treatment options for PD. One such receptor is the metabotropic glutamate receptor 4 ($mGlu_4$), which is located within striato-pallidal synapses and is thought to function presynaptically on GABAergic neurons.[12, 13] Due to its location, it is believed that activation of $mGlu_4$ decrease GABAs release at this synapse, which would, in turn, decrease output of the indirect pathway, and ultimately, reduce or eliminate the PD symptoms.[14, 15] One finding underlying the hypothesis that $mGlu_4$ activation or potentiation might have neuroprotective effects stems from findings that patients undergoing deep brain stimulation

within the indirect pathway, the effect that $mGlu_4$ activation/potentiation is proposed to mimic via a pharmacological mechanism, appear to have a slower disease course, requiring less L-DOPA than cohort of patients who have not been treated with DBS.[16-18] Mechanistically, it has been proposed that $mGlu_4$ potentiation may serve a neuroprotective role via its presynaptic presence at overactive excitatory synapses projecting from the subthalamic nucleus onto the vulnerable dopaminergic neurons in the substantia nigra pars compacta. Valenti *et al.* showed that stimulation of presynaptic $mGlu_4$ at these synapses reduced excessive glutamate release.[19] Battaglia *et al.* and Betts *et al.* further demonstrated that administration of $mGlu_4$ PAMs prevented dopaminergic cell death in the substantia nigra induced by either MPTP or 6-OHDA treatment.[14, 20] Administration of the group III mGlu receptor orthosteric agonist, L-AP4, also was neuroprotective in 6-OHDA models.[21-23] Additionally, administration of an $mGlu_4$ PAM reduced ischemic brain damage[24] and an $mGlu_4$ PAM has also been shown to reduce inflammatory responses in microglia[25], providing another potential mechanism for neuroprotection.

$mGlu_4$ is part of the larger metabotropic glutamate family of receptors (mGlu receptors) which are family C members of the GPCR family.[26-29] There are eight cloned mGlu receptors and these are further subdivided into three sub-classes: group I ($mGlu_1$ and $mGlu_5$), group II ($mGlu_2$ and $mGlu_3$) and group III ($mGlu_4$, $mGlu_6$, $mGlu_7$ and $mGlu_8$).[27] Much work has been published over the past several years describing both orthosteric agonists[30-32] and positive allosteric modulators (PAMs)[33-35] for $mGlu_4$ as novel therapies for PD. A number of PAM *in vivo* tool compounds have been developed (Figure 1), offering evidence that $mGlu_4$ PAMs could be novel, disease-modifying treatment options. The structural classes of molecules are wide-ranging, from triaryl amines, **1**[36], cyclohexyl amides, **2**[37], picolinamides, **3**[38], and pyrazolo[4,3-

b]pyridines, **4**[39, 40], which speaks to the variability in the allosteric binding sites of the receptor. Although much of the work remains in the preclinical stage, recently, Prexton Therapeutics has advanced their lead molecule, **5**, into clinical studies in Europe.[41] Although this is an exciting development in the $mGlu_4$ PAM field, there still remain many fundamental questions surrounding this oxime structural class, and bringing forth multiple structural classes for clinical evaluation is a high priority for the validation of this receptor in the clinic.

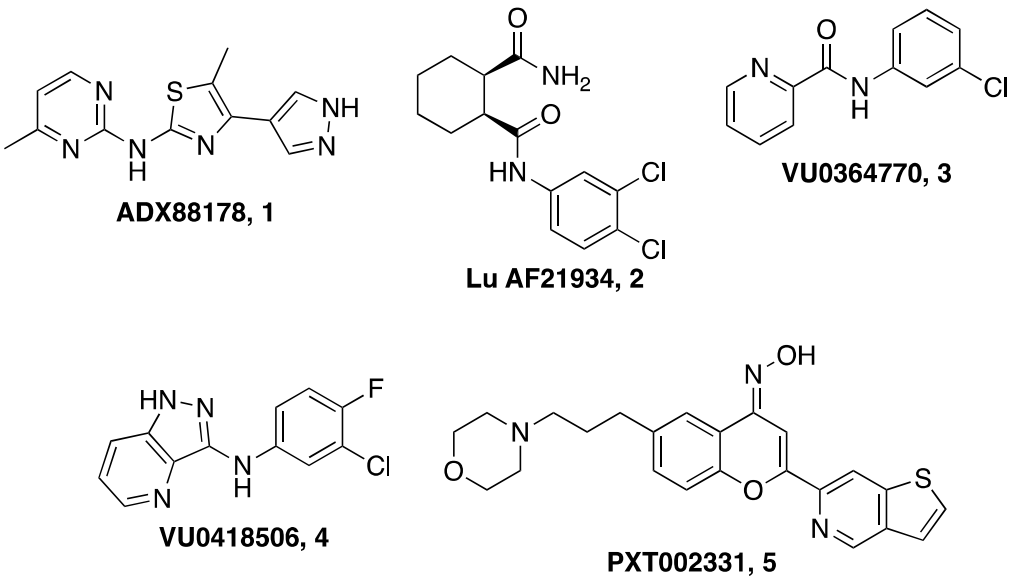

Figure 1. Previously reported $mGlu_4$ PAMs with *in vivo* efficacy in preclinical animal models of PD.

RESULTS AND DISCUSSION

Our laboratory has recently discovered and reported on the pyrazolo[4,3-*b*]pyridine, **4**, structural class as novel, potent and selective $mGlu_4$ PAMs.[39, 40] Unfortunately, this compound class suffered from significant CYP1A2 induction liabilities which led us to develop a new indazole-based scaffold, **6** (Figure 2). These compounds were able to overcome the CYP1A2 induction issues (as measured through upstream AhR activation) noted with **4**; however, metabolic stability remained a liability which was not resolved with this structural change. Thus,

we further evaluated other 6,5-heteroaryl moieties and this report describes our work towards the discovery and characterization of benzo[*d*]isoxazole and benzo[*d*]isothiazole compounds as advanced, preclinical $mGlu_4$ PAMs.

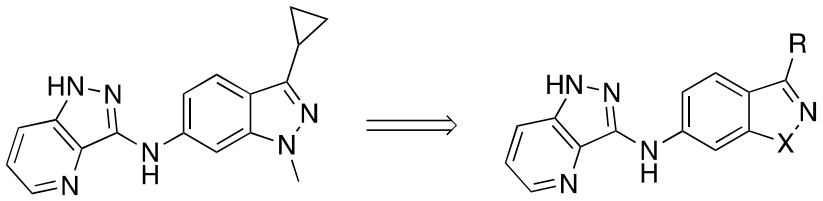

Figure 2. Identification of **6**, an $mGlu_4$ PAM devoid of CYP1A2 induction liability to benzo[*d*]isoxazole and benzo[*d*]isothiazole based PAMs with improved *in vivo* PK properties (CL_p, $t_{1/2}$).

Utilizing the information that was gained during exploration of the indazole scaffold[42], we first investigated simple methyl and ethyl substituted benzo[*d*]isoxazole compounds. The 6-amine-3-alkyl-*N*-methylindazole analogs showed excellent potency and even NH-indazole compounds were active, although there was an ~10-fold loss of potency. As the benzo[*d*]isoxazole does not allow for a substituent in the 1-position (corresponding to the *N*1 of the indazole), we were curious if these analogs would have activity as $mGlu_4$ PAMs. The initial analogs were synthesized as described in Scheme 1, via a palladium-mediated cross coupling of the 3-amino-pyrazolopyridine (or pyrazine) and the appropriately substituted, commercially available benzo[*d*]isoxazole (NaO^tBu, ^{t}BuXPhos, ^{t}BuXPhos palladacycle), followed by deprotection of the PMB group (TFA, μW, 140 ^oC) to yield **10a-j** in low yield.[43]

Scheme 1. Synthesis of first-generation benzo[*d*]isoxazoles.[a]

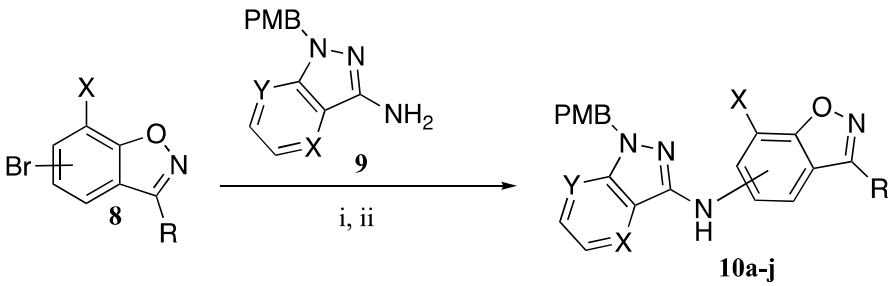

[a]Reagents and conditions: (i) NaO^{t}Bu, ^{t}BuXPhos, ^{t}BuXPhos palladacycle, **9**; (ii) TFA, toluene, 140 °C, μW (4-22% yield, 2 steps).

The SAR around the benzo[*d*]isoxazole started with the 3-methyl-6-substituted analog, **10a**, which showed moderate activity as an mGlu$_4$ PAM (EC_{50} = 1860 nM) (Table 1). Interestingly, the corresponding 3-methyl-5-substitued analog, **10b**, was significantly more active (EC_{50} = 76 nM). The activity for the 5-substituted benzo[*d*]isoxazole was equivalent (or slight loss of potency) regardless of the pyrazolopyridine isomer (**10e**, EC_{50} = 227 nM) or the pyrazolopyrazine (**10d**, EC_{50} = 137 nM). Addition of a fluorine on the pyrazolopyridine moiety also provided an active compound (**10f**, EC_{50} = 219 nM), although there was a loss in potency for for the 6-fluoro analog (**10c**, EC_{50} = 1,570 nM). Addition of a fluorine to the 7-position of the benzo[*d*]isoxazole moiety (**10g-i**) led to an increase in potency, resulting in the most potent compound in the series, **10i** (EC_{50} = 23 nM). Unfortunately, the 5-substituted analogs did not provide any opportunity to improve the compounds as any additional substitution at the 3-position led to reduced (or inactive) activity (e.g., **10j**, EC_{50} = >10,000 nM) – a phenomenon that has been seen in previous work.[42]

Table 1. Structures and activities of new 5- and 6-aminobenzo[*d*]isoxazole analogs.

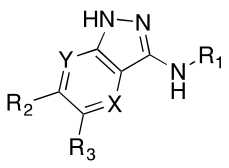

Cmpd	R_1	R_2	R_3	X	Y	$hmGlu_4$ pEC_{50} (± SEM)[a]	$hmGlu_4$ EC_{50} (nM)[a]	%Glu Max (± SEM)[a]
10a	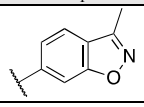	H		N	CH	5.73 ± 0.03	1860	86 ± 18
10b	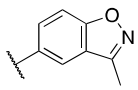	H		N	CH	7.12 ± 0.02	75.9	91 ± 3
10c		F	H	N	CH	5.80 ± 0.36	1,570	80.6 ± 15.1
10d		H		N	N	6.86 ± 0.06	137	85.4 ± 15.8
10e		H		CH	N	6.64 ± 0.06	227	81.9 ± 12.9
10f		H	F	CH	N	6.66 ± 0.02	219	54 ± 3
10g	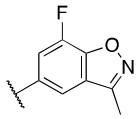	H		N	CH	6.56 ± 0.21	274	77.7 ± 18.1
10h		H		CH	N	6.91 ± 0.16	122	74.7 ± 17.4
10i		H		N	N	7.64 ± 0.03	22.9	70 ± 3
10j	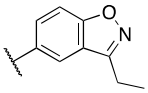	H		CH	N	<5.00	>10,000	54 ± 11

[a]For assay conditions, see Experimental Section.

Although the SAR was limited around the 5-substituted benzo[*d*]isoxazole framework, we evaluated these compounds in a battery of Tier 1 *in vitro* DMPK assays (Table 2). All of the compounds evaluated displayed moderate/high predicted hepatic clearance in human microsomes (Q_H = >50%) and more moderate clearance in rat microsomes (Q_H <50%). In addition, the compounds had good plasma free fraction (%f_u ~3–8%) in both species. Unfortunately, these small, aromatic compounds were potent CYP1A2 inhibitors (<700 nM), and showed significant CYP1A2 induction (AhR activation = E_{max} >50, data not shown). The rat and human $mGlu_4$ in vitro potency data tracked well, which is common with most of the $mGlu_4$ PAM scaffolds that we have identified. Lastly, since the *in vitro* rat liver microsome clearance data indicated that these compounds would be moderately cleared, we wanted to establish an *in vitro/in vivo* correlation (IV/IVC) for this initial scaffold. The compounds were investigated using a rat IV cassette dosing strategy to evaluate their *in vivo* pharmacokinetic properties, including clearance and half-life.[44] As can be seen in Table 2, these compounds were all highly

cleared, with the exception of **10d**. However, the $t_{1/2}$ was not ideal (<90 min; MRT <60 min) for all of the compounds; therefore, none were progressed further into *in vivo* efficacy studies.

Table 2. *In vitro* DMPK and rat potency data of benzo[*d*]isoxazole analogs.

Cmpd	Human[a] (mL/min/kg)		Rat[a] (mL/min/kg)		Plasma protein binding (%f_u)		CYP1A2 (μM)	Rat $mGlu_4$ EC_{50} (nM); %Glu Max[d]
	CL_{INT}	CL_{HEP}	CL_{INT}	CL_{HEP}	Human	Rat		
10b	14.8	8.7	31.8	21.9	6.2	5.8	<0.1	95.5; 104.8
10c	24.2	11.3	33.4	22.6	5.4	7.6	<0.1	123; 111.3
10d	114	17.7	3.0	2.9	6.6	6.4	0.2	65.0; 126.8
10e	81.4	16.7	30.1	21.0	6.6	7.9	0.7	209; 107.7
10f	23.6	11.1	39.3	25.2	5.4	4.4	0.5	190; 120.6
10g	31.1	12.5	66.4	34.1	2.9	5.0	<0.1	53.0; 113.8
10h	50.2	14.8	110	42.7	2.8	3.3	<0.1	169; 113.6

[a]Intrinsic and predicted hepatic clearance based on experiments in liver microsomes. [b]%f_u = % fraction unbound. [c]IC_{50} determination of CYP1A2 enzyme inhibition in human liver microsomes using specific probe substrate-metabolite pairs. [d]Thallium-flux $mGlu_4$ assay.

In vivo PK – Rat Cassette IV Clearance

	CL (mL/min/kg)	Vss (L/kg)	MRT (min)	$t_{1/2}$ (min)
10c	64.6	2.0	31.6	54.8
10d	24.3	0.9	37.2	28.6
10e	38.0	2.5	60.6	106.7
10g	81.1	3.1	38.4	31.2
10h	30.5	1.2	38.0	34.7

Since the introduction of a benzo[*d*]isoxazole ring system was productive in terms of potency, we next wanted to evaluate the 6-benzo[*d*]isoxazole-3-substituents to assess the impact on potency, PK and CYP1A2 inhibition. Previously, we showed that extending the steric bulk in this portion of the indazole scaffold led to more potent compounds, and, importantly, improved CYP1A2 profiles. The generation of these analogs is shown in Schemes 2 and 3.

The synthesis of the 3-alkylsubstituted benzo[*d*]isoxazole analogs started with the commercially available 3-bromophenol, **11**, which was acylated under Friedel-Crafts conditions ($AlCl_3$, RCOCl, reflux) to yield **13** in moderate yield. Next, the resulting ketone was converted to the imine, **14** (7M NH_3 in MeOH), which was then subjected to NCS-mediated ring closure

(NCS, K_2CO_3, THF) to yield the penultimate intermediate, **15**.[45] The final targets (**16a-o**) were synthesized via palladium-catalyzed cross-coupling of the 3-aminopyrazolopyridine analogs, **9**, (NaO^tBu, ^{t}BuXPhos, ^{t}BuXPhos palladacycle) followed by deprotection of the PMB group (TFA, μW).[43]

Scheme 2. Synthesis of 6-benzo[*d*]isoxazole-3-alkyl analogs.[a]

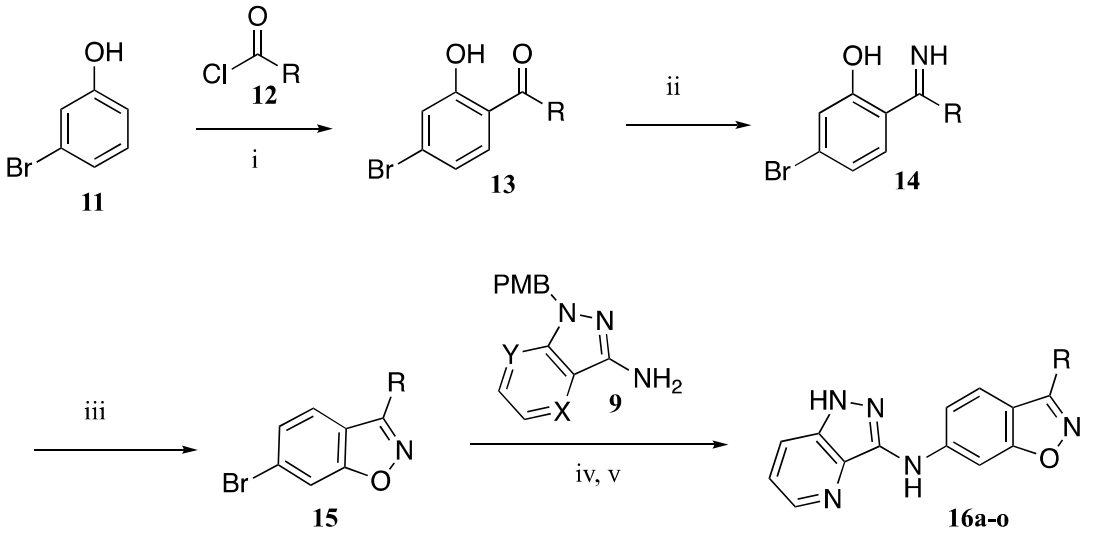

[a]Reagents and conditions: (i) $AlCl_3$, dichloroethane, reflux (53-89%); (ii) 7M NH_3 in MeOH; (iii) NCS, K_2CO_3, THF, rt; (iv) NaO^tBu, ^{t}BuXPhos, ^{t}BuXPhos palladacycle, **9**; (v) TFA, toluene, 140 ^oC, μW (5-63%, 2 steps).

The difluoroethyl analog, **16p**, was synthesized as outlined in Scheme 3. The commercially available ethyl 6-bromobenzo[*d*]isoxazole-3-carboxylate, **17**, was reacted with MeMgBr (THF, -78 ^oC) to yield the ketone, **18**. The ketone, **18**, was converted to the 1,1-difluoroethyl analog, **19**, via treatment with DAST (dichloroethane, 90 ^oC). The final compound, **16p**, was realized after palladium-catalyzed cross-coupling of **9** and **19** (Xantphos, Cs_2CO_3, μW) under microwave irradiation followed by PMB-deprotection (TFA, μW).[43]

Scheme 3. Synthesis of difluoroalkyl analog, **16p**.[a]

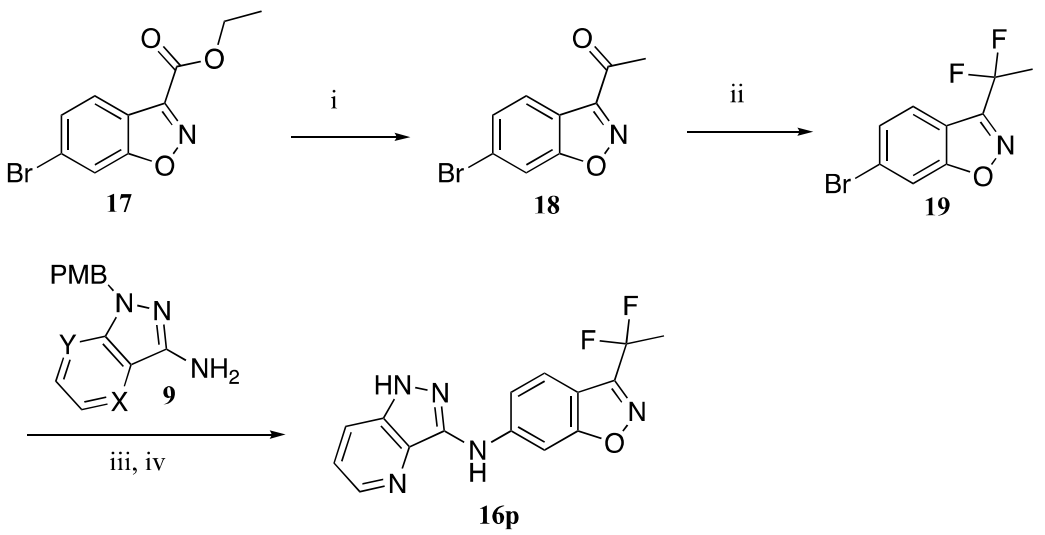

[a]Reagents and conditions: (i) MeMgBr, THF, -78 °C (85% yield); (ii) DAST, dichloroethane, 90 °C, 3 h (69% yield); (iii) $Pd_2(dba)_3$, Xantphos, Cs_2CO_3, 1,4-dioxane, **9**, μW, 140 °C, 2 h; (iv) TFA, μW, 150 °C, 30 min (18% yield, 2 steps).

Extension of the methyl group to an ethyl group, **16a**, resulted in similar potency (EC_{50} = 1350 nM vs. **10a**, EC_{50} = 1860 nM). Further increase in steric bulk to the isopropyl led to an ~2-fold improvement in potency, **16b** (EC_{50} = 575 nM). Introduction of small, cycloalkyl groups was productive and led to compounds that were equipotent with the isopropyl analog (**16c-f**); however, moving the pyridine around the pyrazolopyridine head group led to a compound with much reduced potency (**16g**, EC_{50} = 2,400 nM). Moving the branching point further from the ring system did not improve the potency (**16h-k**). Again, moving the nitrogen of the pyrazolopyridine around the ring led to a reduction in potency (**16k**, EC_{50} = 2,820 nM). Introduction of longer, branched alkyl groups was a productive change and led to the most potent compounds in the benzo[*d*]isoxazole series. The 3-(pentan-3-yl)benzo[*d*]isoxazoles were potent $mGlu_4$ PAMs (**16l**, EC_{50} = 98 nM; **16m**, EC_{50} = 129 nM) and, like the previous example, the pyrazolo[3,4-*b*]pyridine isomer was much less active (**16n**, EC_{50} = 525 nM). The 3-(pentan-2-yl) analog retained much of the activity (**16o**, EC_{50} = 117 nM) as the racemate. Lastly, as metabolic hot-spot analysis revealed the methylene (or methine) of the 3-substituted (cyclo)alkyl

substituents as a potential site of metabolism, we synthesized the 3-(1,1-difluoroethyl) derivative in order to block this site. The difluoroethyl analog was slightly more potent than the corresponding ethyl analog (**16p**, EC_{50} = 678 nM vs. **16a**, EC_{50} = 1350 nM).

Table 3. Structures and activities of select 6-amino-3-alkylbenzo[*d*]isoxazole analogs.

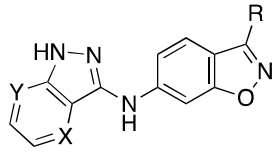

Cmpd	R	X	Y	$hmGlu_4$ pEC_{50} (± SEM)[a]	$hmGlu_4$ EC_{50} (nM)[a]	%Glu Max (± SEM)[a]
16a		N	CH	5.87 ± 0.03	1350	72 ± 4
16b		N	CH	6.24 ± 0.01	575	23 ± 1
16c		N	N	6.15 ± 0.04	708	102 ± 11
16d		N	CH	6.07 ± 0.01	851	88 ± 11
16e		N	N	6.29 ± 0.07	514	85.5 ± 23.1
16f		N	CH	6.14 ± 0.11	723	87.6 ± 22.0
16g		CH	N	5.62 ± 0.01	2400	60 ± 7
16h		N	CH	6.09 ± 0.03	813	53 ± 2
16i		N	N	6.07 ± 0.12	860	83.5 ± 13.2
16j		N	CH	5.89 ± 0.25	1,300	68.9 ± 9.5
16k		CH	N	5.55 ± 0.03	2820	84 ± 5
16l		N	N	7.01 ± 0.01	98	106 ± 3
16m		N	CH	6.89 ± 0.02	129	92 ± 2
16n		CH	N	6.28 ± 0.005	525	97 ± 2
16o		N	CH	6.93 ± 0.04	117	92 ± 3
16p		N	CH	6.17 ± 0.01	678	58.8 ± 15.1

[a]For assay conditions, see Experimental Section.

This new set of 3-alkyl-6-benzo[*d*]isoxazole analogs were evaluated in Tier 1 *in vitro* DMPK assays as well as *in vivo* rat PK assays (Table 4). Most of the compounds that were

evaluated showed high intrinsic (and high predicted hepatic) clearance in both human and rat liver microsomes (Q_H >50%). It should be noted that introduction of the difluoroethyl group significantly reduced the intrinsic clearance, especially in rat liver microsomes (**16p**). Introduction of the extended (cyclo)alkyl groups in the 3-position led to a reduction across the board in plasma free fraction, as compared to the simple 3-methyl compounds (Table 2). However, the level of CYP1A2 inhibition was significantly reduced – mimicking the trend that we previously reported. In addition, many of these compounds had reduced AhR activation (**16i** (VU0652264), AhR activation = 6.4). A selection of these compounds was evaluated *in vivo* in a rat IV cassette clearance experiment.[44] The compounds were moderately cleared; however, they showed good CNS penetration when evaluated in a rat cassette plasma:brain distribution assay (**16i**, K_p = 4.7).

Table 4. *In vitro* and *in vivo* DMPK for 6-amino-3-alkylbenzo[*d*]isoxazole analogs.

	Human (mL/min/kg)		Rat (mL/min/kg)		Plasma unbound (%f_u)		CYP1A2 (μM)	Rat $mGlu_4$ EC_{50} (nM); %GluMax
Cmpd	CL_{INT}	CL_{HEP}	CL_{INT}	CL_{HEP}	Human	Rat		
16a	69.9	16.1	204	52.1	2.7	3.7	<0.1	ND
16d	83.2	16.8	1219	66.2	2.6	1.6	1.8	ND
16e	42.3	14.0	281	56.0	1.3	0.8	3.0	518; 101.9
16f	30.7	12.5	398	59.5	1.0	0.7	1.2	680; 97.9
16i	7.2	5.4	62.5	33.0	2.3	2.3	3.2	501; 98.7
16j	7.3	5.4	86.9	38.8	1.6	2.2	1.1	542; 84.8
16m	84.2	16.8	488	61.2	0.9	1.9	1.0	ND[e]
16p	24.6	11.3	11	9.5	0.3	1.7	0.5	1600; 83.8

[a]Intrinsic and predicted hepatic clearance based on experiments in liver microsomes. [b]%f_u = % fraction unbound. [c]IC_{50} determination of CYP1A2 enzyme inhibition in human liver microsomes using specific probe substrate-metabolite pairs. [d]Thallium-flux $mGlu_4$ assay. [e]ND = not determined

In vivo PK

	Rat IV Cassette			Cassette PBL		
Cmpd	CLp (mL/min/kg)	$t_{1/2}$ (min)		Plasma (ng/mL)	Brain (ng/g)	K_p
16e	23.2	45.9		117	145	1.2
16f	62.1	100.0		ND	ND	N/A
16i	37.8	87.4		60.5	285	4.7
16j	43.2	79.9		ND	ND	N/A
16p	27.8	90.8		ND	ND	N/A

To further establish that the reduction in the AhR activation improved the overall PK profile of the scaffold, we initiated a subchronic, 4-day repeat dosing PK study with **16i** (Table 5A). This compound was dosed once-daily (15 mg/kg, PO) for four days and the plasma levels were evaluated on days 1 and 4. Unlike **4**, for which we saw a significant reduction in plasma exposure at day 4, C_{max} and AUC levels of **16i** were comparable at both day 1 (C_{max} = 86.3 ng/mL; AUC = 624 hr·ng/mL) and day 4 (C_{max} = 62.8 ng/mL; AUC 690 hr·ng/mL). This result suggests that by reducing the AhR activation, we would be able to identify, and potentially develop, an $mGlu_4$ PAM that would be suitable for chronic dosing applications.

Next, we evaluated **16i** for its ability to reverse haloperidol-induced catalepsy in a preclinical rodent model of PD (Table 5B).[46] In this model, male Sprague-Dawley rats were randomly assigned to treatment groups and injected with haloperidol (0.75 mg/kg i.p.) and returned to their home cages for 60 min. Vehicle, **16i** (10mg/kg) or **4** (10mg/kg) were administered orally 30 minutes prior to testing for catalepsy (N = 11 – 12 rats/group). As shown in Table 5B, **16i** exhibited a robust reversal of cataleptic activity in this model after oral administration (One-way ANOVA: $F_{2,32} = 26.9$, $p < 0.0001$) – similar to previously evaluated $mGlu_4$ PAMs (**4**, Table 5B). To better understand this *in vivo* efficacy (PK/PD), we quantified the plasma, brain and cerebrospinal fluid (CSF) levels of **16i** from the PD study. As shown in Table 5C, the reversal of HIC was observed with CSF levels of 627 nM, levels equivalent to the rat $mGlu_4$ EC_{50}.

Table 5. Subchronic PK dosing of **16i** and *in vivo* efficacy studies.

A Chronic dosing of **16i**, (15 mg/kg, PO) **B** Haloperidol efficacy

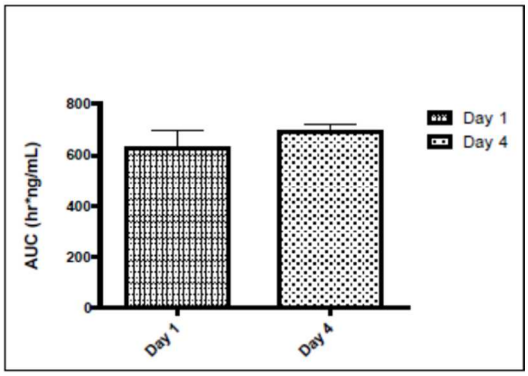

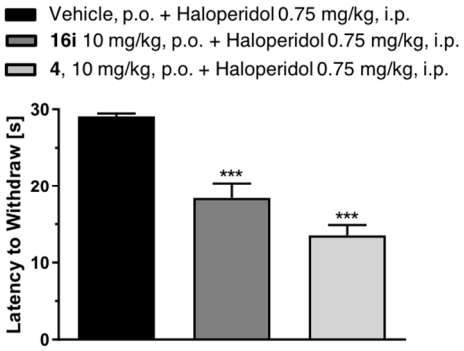

Statistics: **16i** reversal of Haloperidol-induced Catalepsy in male Sprague-Dawley rats. One-way ANOVA: $F_{2,32} = 26.9$, $p < 0.0001$. ***$p < 0.0001$ vs. Vehicle + Haloperidol (Dunnett's multiple comparison test). N = 11 – 12 rats/group.

C

In vivo exposure in rat plasma/brain after PO administration in haloperidol-induced catalepsy					
Dose	Plasma (nM)	Free Plasma (nM)	Brain (nM)	Free Brain (nM)	CSF (nM)
10 mg/kg	450	11.2	958	5.8	627

Although we have identified compounds that mitigate the CYP1A2 liability, there still remained issues with modest potency and high clearance *in vivo* and short $t_{1/2}$ in rats. Thus, we next turned our attention to moving from the benzo[*d*]isoxazole scaffold to the benzo[*d*]isothiazole scaffold in an attempt to probe the ring size of the five-membered annulated ring system. As larger substituents on the 3-position of the benzo[*d*]isoxazole group were productive in reducing the CYP1A2 inhibition, we started with these same groups for evaluation. As these moieties were not commercially available, significant synthetic chemistry effort was devoted to making the appropriate analogs and these efforts are outlined in Schemes 4–9.

The synthetic procedure for the 3-alkyl-6-bromobenzo[*d*]isothiazole or 3-alkyl-6-bromoisothiazolo[4,5-*b*]pyridine analogs (e.g., **27a-i**) is shown in Scheme 4. The commercially available 4-bromo-2-fluorobenzaldehyde, **20**, was converted to the secondary alcohol, **21,** via reaction with the appropriate alkyl Grignard. The alcohol was oxidized to the key intermediate ketone, **22**, using Dess-Martin periodinane. The isothiazolo[4,5-*b*]pyridine analogs were synthesized in an analogous manner starting with the 5-bromo-3-fluoropicolinonitrile, **23**, which

was reacted with the alkyl Grignard to yield **24**. Both **22** and **24** were carried forward under the same reaction conditions. Thus, they were reacted with BnSH under basic conditions to yield the benzylthio derivative, **25**. The ring closure to the isothiazole ring system was completed using SO_2Cl_2 and NH_3 to yield **26**.[47] The final compounds, **27a-i**, were made via the palladium-catalyzed cross-coupling with **9** followed by deprotection as detailed above.[43]

Scheme 4.

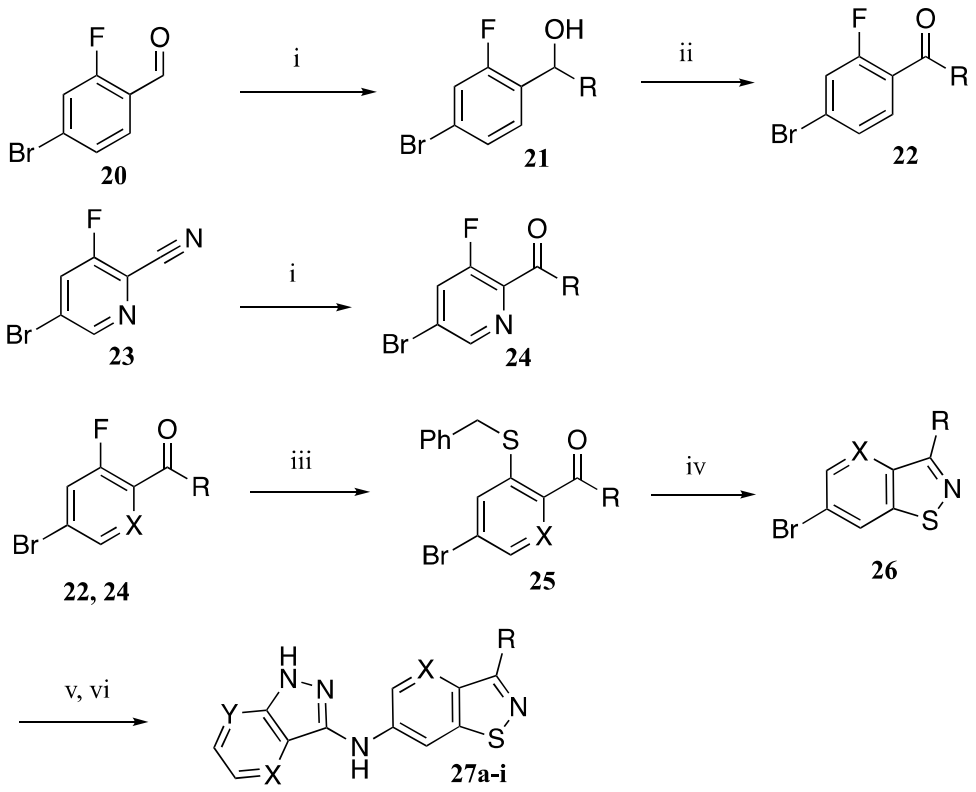

[a]Reagents and conditions: (i) RMgBr, THF, 0 °C to rt, 24 h; (ii) DMP, CH_2Cl_2, rt, 1 h; (iii) BnSH, ^{t}BuOK, THF, rt, 1.5 h; (iv) SO_2Cl_2, 7M NH_3 in MeOH, dichloroethane, 1.5 h (28-82% yield, 4 steps); (v) ^{t}BuONa, Pd precatalyst, ^{t}BuXPhos, ^{t}BuOH, 9, 60 °C, 2 h; (vi) TFA 150 °C, 15 min, μW, (9-47% yield, 2 steps).

The trifluoromethyl analog, **27j**, was synthesized in a similar manner to the previous compounds with a reversal of some of the steps. Thus, **20** was reacted with BnSH (NaO^tBu, THF) to yield **28**. Next, the aldehyde was converted to the trifluoromethyl ketone via a two-step

procedure starting with trifluoromethyl addition (TMS-CF_3, TBAF, 0 ^oC) to yield the secondary alcohol which was oxidized to the ketone, **29**, with Dess-Martin periodinane. The thio-ketone was cyclized to the isothiazole (SO_2Cl_2, rt) followed by the reaction with ammonia (7M in MeOH) to yield **30**.[47] Finally, the target compound, **27j**, was synthesized as described above under palladium catalysis/deprotection conditions.[43]

Scheme 5.

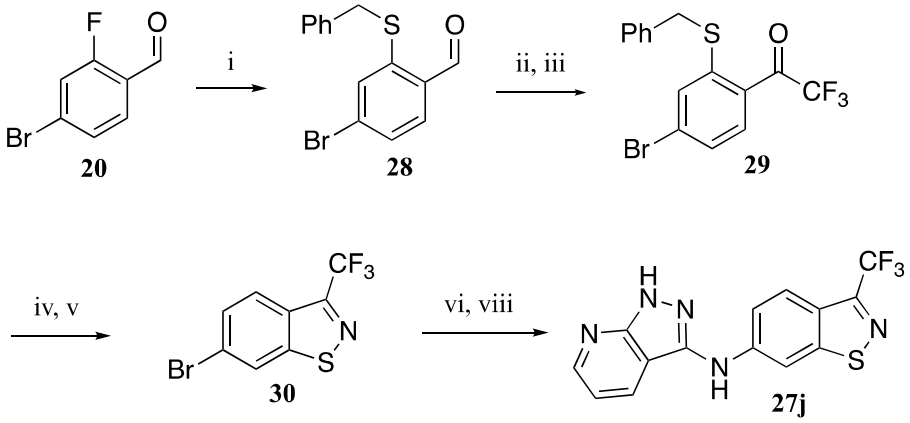

[a]Reagents and conditions: (i) BnSH, NaO^{t}Bu, THF (37%) (ii) TMF-CF_3, TBAF, 0 ^oC, THF; (iii) DMP, CH_2Cl_2, rt, 1 h (99%); (iv) SO_2Cl_2, rt, dichloroethane; (v) NH_3, rt, THF (4%, 2 steps); (vi) ^{t}BuONa, ^{t}BuXPhos palladacycle, ^{t}BuXPhos, 9; (vii) TFA 150 ^oC, 15 min, μW (29%, 2 steps).

Compound **31** was coupled ($Pd_2(dba)_3$, Xantphos, Cs_2CO_3) with the PMB-protected pyrazolo[4,3-*b*]pyridine-3-amine, **9**, to give the desired compound **32** in modest yield. The ethyl ester, **32**, was converted to the methyl ketone, **33**, via reaction with MeMgBr (-78 ^oC, THF), followed by PMB-deprotection (TFA:toluene, 150 ^oC, μW) in good yield. The final tertiary alcohol, **27k**, was obtained in low yields via another addition of MeMgBr to the methyl ketone.

Scheme 6.

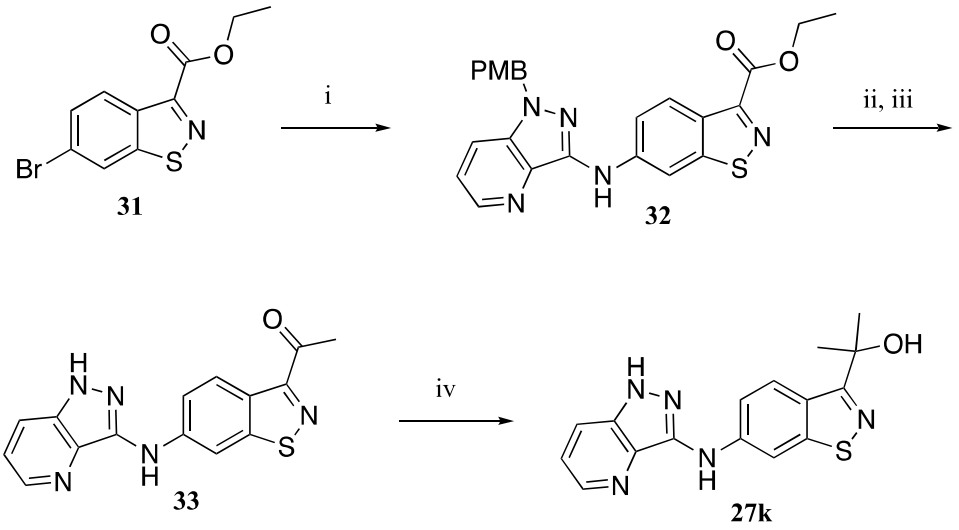

[a]Reagents and conditions: (i) $Pd_2(dba)_3$, Xantphos, Cs_2CO_3, 1,4-dioxane, 140 °C, μW, **9** (42 -46% yield); (ii) MeMgBr, -78 °C, THF; (iii) TFA:toluene (1:1), 150 °C, μW, 30 min (69% yield, 2 steps); (iv) MeMgBr, THF, -78 °C (13%).

The synthesis of the amide analogs (**27n-v**) is shown in Scheme 7. Starting from **32**, the carboxylic acid **34** was realized by saponification of the ester (LiOH, MeOH). Next, the amides, **27n-v**, were synthesized via coupling with the appropriate amine under HATU conditions (DIEA, DMF) followed by PMB-deprotection in low to moderate yield over the three steps.

Scheme 7.

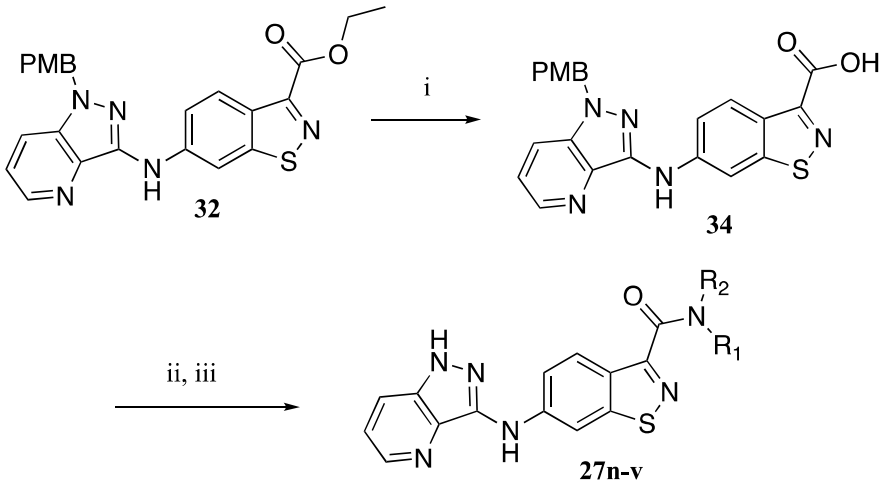

[a]Reagents and conditions: (i) LiOH (aq), MeOH, 1,4-dioxane; (ii) NHR_1R_2, DIEA, HATU, DMF; (iii) TFA, 150 °C, μW (4-55% yield, 3 steps)

The preparation of the 3-acylpiperidine analogs, **27l,m**, is shown in Scheme 8. The 1-bromo-3-fluorobenzene starting material, **38**, was acylated with **39** under Friedel-Crafts conditions ($AlCl_3$, 80 ^oC) to give **40** in low yield. Next, **40**, was reacted with benzylthiol displacing the fluorine to yield the isothiazole precursor, **41**. The isothiazole was synthesized as previously described by reacting the 2-benzylthio ketone with sulfuryl chloride followed by the addition of ammonia which gave the cyclized isothiazole **42** in 55% yield over three steps.[47] Finally, the target compounds, **27l-m**, were synthesized by palladium-catalyzed cross-coupling followed by PMB-deprotection in good yield.[43]

Scheme 8.

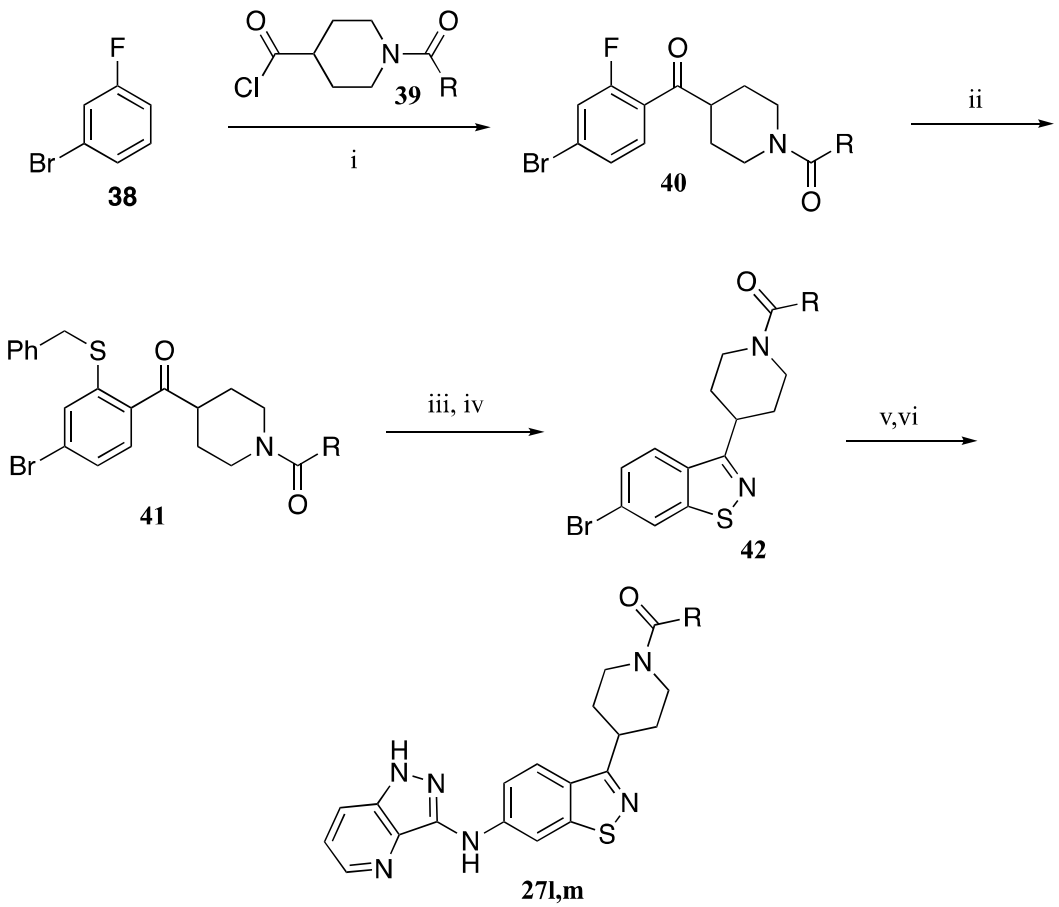

[a]Reagents and conditions: (i) $AlCl_3$, 80 °C (21%); (ii) BnSH, ^{t}BuOK, THF, rt; (iii) SO_2Cl_2, dichloroethane, rt; (iv) 7M NH_3 in MeOH, THF, rt (55% yield, 3 steps); (v) NaO^{t}Bu, ^{t}BuXPhos, ^{t}BuXPhos palladacycle, 9; (vi) TFA, toluene, 150 °C, μW (69% yield, 2 steps).

Lastly, the tertiary amine analog, **27w**, was synthesized as outlined in Scheme 9. The starting material, **35**, which was made as outlined in Scheme 4 for **26**, was mono-brominated on the 3-methyl position (NBS, benzoylperoxide, CCl_4) to yield **36**.[48] The newly made 3-bromomethyl was displaced by 4,4-difluoropiperidine (NMP, μW, 150 °C) to give the penultimate intermediate, **37** in 27% yield over two steps.[48] The final compound, **27w**, was completed via palladium-catalyzed cross-coupling with **9** as outlined above, followed by PMB-deprotection in 43% yield over the two steps.[43]

Scheme 9.

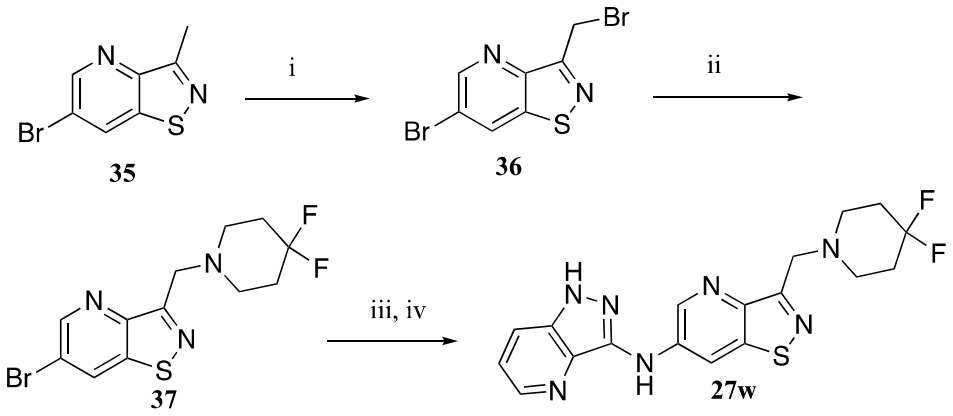

[a]Reagents and conditions: (i) NBS, benzoylperoxide, CCl_4, reflux; (ii) 4,4-difluoropiperidine, NMP, 150 °C, (27% yield, 2 steps); (iii) NaO^{t}Bu, ^{t}BuXPhos, ^{t}BuXPhos palladacycle, 9; (iv) TFA, toluene, 150 °C, μW (43% yield, 2 steps).

Having established synthetic procedures to access the required analogs, we evaluated the new analogs in the human $mGlu_4$ potency assay (Table 6). Utilizing the knowledge gained from the benzo[*d*]isoxazole series, we started with sterically hindered 3-alkyl groups since these, generally, gave the best CYP1A2 induction profile. The pyrazolo[4,3-*b*]pyridine analog, **27a** (EC_{50} = 269 nM), led to an ~2-fold increase in potency compared to the benzo[*d*]isoxazole analog, **16j**. Addition of a nitrogen to the benzo[*d*]isothiazole ring system, **27b**, led to a significant increase in potency (EC_{50} = 74 nM). The pyrazolo[3,4-*b*]pyridine regioisomer, **27c**, resulted in a reduction in potency of ~3-fold compared to **27a** (EC_{50} = 759 nM). The pyrazolo[3,4-*b*]pyrazine with a nitrogen in the benzo[*d*]isothiazole system was also a potent compound (**27d**, EC_{50} = 105 nM). In general, the benzo[*d*]isothiazole ring system was significantly more potent than the corresponding benzo[*d*]isoxazole scaffold. Examples of this increase in potency can be seen in a number of analogs, such as **27e** (EC_{50} = 40 nM) vs. **16a** (EC_{50} = 1350 nM). In addition, the trend of the pyrazolo[3,4-*b*]pyridine leading to a loss of potency was continued for the ethyl substituent, **27f** (EC_{50} = 102 nM). Small cycloalkyl groups were well tolerated (**27g,h**) as well as bulkier groups such as *tert*-butyl (**27i**); however, the 3-

trifluoromethyl, **27j**, was less active (EC_{50} = 794 nM). The tertiary alcohol was synthesized to introduce a group that may improve the water solubility; however, this moiety was much less active (**27k**, EC_{50} = 1,050 nM). To further explore the functional group tolerance off the 3-position, we made acylated piperidine analogs, **27l,m**, which retained activity (EC_{50} = 200 and 389 nM, respectively). Next, we turned to the amide moiety which proved to be a fruitful functional group in the indazole series. A variety of secondary and tertiary amides were synthesized (**27n-v**) and evaluated. The 3,3-difluoropyrrolidine analog, **27n**, was active (EC_{50} = 331 nM); however, potency was improved by expanding the ring to the 6-membered piperidine (4,4-difluoropiperidine), **27r** (EC_{50} = 52 nM). However, other 6-membered tertiary amides were not as potent (**27s-v**), suggesting the gem-difluoro moiety is important in the binding. The most potent amides that were investigated with the secondary 3,3-difluorocyclobutane derivatives **27o** (EC_{50} = 50 nM) and **27p** (EC_{50} = 26 nM) being the most potent analogs. Methylation of the secondary amide was productive and led to an equivalent compound in terms of potency (**27q**, EC_{50} = 68 nM). Removal of the amide group, resulting in the tertiary amine compound, **27w** (EC_{50} = 81 nM) was active; however, all of these amine compounds that were synthesized suffered from very high *in vitro* liver microsomal clearance (data not shown).

Table 6. Structures and activities of 6-amino-3-substituted benzo[*d*]isothiazole analogs.

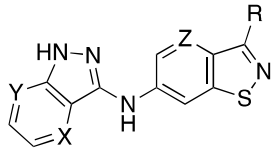

Cmpd	R	X	Y	Z	hmGlu$_4$ pEC$_{50}$ (± SEM)[a]	hmGlu$_4$ EC$_{50}$ (nM)[a]	%Glu Max (± SEM)[a,b]
27a		N	CH	CH	6.57 ± 0.04	269	70 ± 2
27b		N	CH	N	7.13 ± 0.01	74	51 ± 3
27c		CH	N	CH	6.12 ± 0.04	759	74 ± 1
27d		N	N	N	6.98 ± 0.05	105	54 ± 4
27e		N	CH	CH	7.40 ± 0.07	40	77 ± 4

27f		CH	N	CH	6.99 ± 0.05	102	57 ± 4
27g	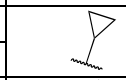	N	CH	CH	7.09 ± 0.02	81	76 ± 4
27h		N	N	CH	7.17 ± 0.04	68	73 ± 3
27i		N	CH	CH	6.49 ± 0.08	324	64 ± 5
27j	CF_3	CH	N	CH	6.10 ± 0.04	794	50 ± 4
27k		N	CH	CH	5.98 ± 0.09	1050	98 ± 8
27l	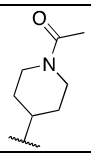	N	CH	CH	6.70 ± 0.05	200	79 ± 4
27m	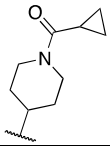	N	CH	CH	6.41 ± 0.04	389	111 ± 6
27n	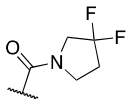	N	CH	CH	6.48 ± 0.01	331	92 ± 7
27o	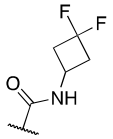	N	CH	CH	7.30 ± 0.08	50.1	50.5 ± 7.5
27p		N	N	CH	7.58 ± 0.07	26.0	68.1 ± 15.6
27q	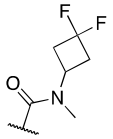	N	CH	CH	7.17 ± 0.21	68.1	76.7 ± 17.6
27r	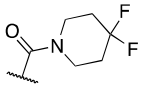	N	CH	CH	7.28 ± 0.06	52.4	71.0 ± 16.6
27s	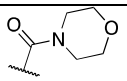	N	CH	CH	6.56 ± 0.05	275	62 ± 12
27t	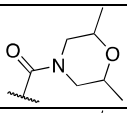	N	CH	CH	6.49 ± 0.06	324	44 ± 9
27u	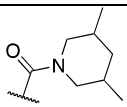	N	CH	CH	6.35 ± 0.03	447	63 ± 3
27v	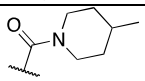	N	CH	CH	6.40 ± 0.04	398	80 ± 2
27w	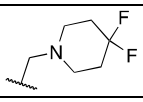	N	CH	N	7.09 ± 0.05	81	84 ± 6

[a]For assay conditions, see Experimental Section.

These new benzo[*d*]isothiazole analogs were evaluated in a battery of Tier 1 *in vitro* DMPK assays (Table 7). Although many of the compounds showed moderate clearance in human liver microsomes (CL_{HEP}), they were more highly cleared in rat liver microsomes (e.g., **27b**). As noted above, **27w**, was highly cleared in rat liver microsomes and was unstable in rat plasma, which was a common trend in all of the amines that were synthesized for the project. The plasma protein binding was high to moderate for all compounds that were evaluated, with no clear trend emerging. The CYP1A2 inhibition was also examined and showed a similar trend to previously reported scaffolds. The 3-neopentyl derivatives (**27b,d**) showed significantly reduced inhibition of the CYP1A2 enzyme; however, the smaller 3-cyclopropyl (**27g,h**) group did show nanomolar inhibition (similar to what was seen in the indazole scaffold). As the substitution at the 3-position increased in size, the CYP1A2 inhibition decreased and all of the amides that were tested did not show any inhibition of the enzyme (>30 μM). In fact, **27o**, was inactive against all CYP enzymes studied (CYP1A2, 3A4, 2C9, 2D6: >30 μM). Lastly, the two amide compounds (**27o,p)** were the most potent against the rat $mGlu_4$ receptor (~82 nM).

Table 7.

Cmpd	Human (mL/ming/kg)		Rat (mL/min/kg)		Plasma protein binding (%f_u)		CYP1A2 (μM)	Rat $mGlu_4$ EC_{50} (nM); %GluMax
	CL_{INT}	CL_{HEP}	CL_{INT}	CL_{HEP}	Human	Rat		
27b	24.7	11.4	277	55.9	0.6	1.6	22.1	ND[e]
27d	40.2	13.8	189	51.1	1.3	1.1	>30	158; 112.3
27e	35.4	13.2	127	45.1	3.5	3.0	ND[e]	ND[e]
27g	28.9	12.2	176	50.1	0.9	1.4	0.4	ND[e]
27h	41.2	13.9	59.4	32.1	1.2	0.8	0.7	ND[e]
27l	15.8	9.00	21.0	16.2	4.2	3.9	21.7	166; 98.9
27o	19.0	10.0	34.2	23.0	2.4	0.5	>30	82.7; 76.8
27p	2.60	2.30	8.30	7.40	0.4	0.7	>30	82.2; 86.6
27q	298	19.6	2938	68.4	0.6	<0.1	ND[e]	ND[e]
27r	54.0	15.1	393	59.4	2.1	2.9	>30	139; 102.8
27s	44.3	14.2	172	49.8	7.7	5.9	ND[e]	ND[e]
27t	60	15.6	229	53.6	1.3	3.4	ND[e]	ND[e]
27w	27.5	11.9	1085	65.8	[f]	[f]	>30	ND[e]

[a]Intrinsic and predicted hepatic clearance based on experiments in liver microsomes. [b]%f_u = % fraction

unbound. [c]IC_{50} determination of CYP1A2 enzyme inhibition in human liver microsomes using specific probe substrate-metabolite pairs. [d]Thallium-flux $mGlu_4$ assay. [e]ND = not determined. [f]unstable

Next, based on their overall profile (potency, *in vitro* DMPK), a select few compounds were chosen for administration in a rat cassette to determine the plasma:brain partition ratio (Table 8).[44] All of the compounds evaluated showed excellent plasma levels; however, only one compound, **27o**, showed appreciable brain levels (K_p = 0.4). Very minor changes to the structure, such as the pyrazolo[4,3-*b*]pyrazine, **27p** (K_p = 0.08) and the methylated amide, **27q** (K_p = BLQ), led to a significant reduction in brain penetration. Since the K_p of **27o** was acceptable, we next evaluated this compound in a rat IV cassette experiment for *in vivo* plasma clearance and half-life (Table 8). This IV dosed experiment showed that **27o** was a low clearance compound in rat (CL_p = 3.1 mL/min/kg) with an excellent half-life ($t_{1/2}$ = 445 min).

Table 8. *In vivo* cassette plasma:brain evaluation and IV PK cassette study for select compounds.

Cassette PBL			
	Plasma (ng/mL)	Brain (ng/g)	K_p
27o	284	107	0.4
27p	690	55.6	0.08
27q	511	BLQ	N/A
27r	249.0	35.5	0.14

Rat IV Cassette Clearance, **27o**	
CL_p (mL/min/kg)	3.1
V_{ss} (L/kg)	1.6
$t_{1/2}$ (min)	445
MRT (min)	510

The difluorocyclobutane, **27o**, was evaluated in our mGlu selectivity panel and it was inactive against all seven members of the mGlu receptor family (Table 9). In addition, we sent the compound for a larger selectivity panel screen (Eurofins Lead Profiling), which is a panel of

~70 GPCRs, transporters, and ion channels.[49] The results show that **27o** is a selective compound as the only receptor that was identified was Adenosine A_3 (76% inhibition of radioligand binding at 10 μM).

Table 9. Selectivity of **27o**.

Cmpd	$hmGlu_1$	$rmGlu_2$	$rmGlu_3$	$rmGlu_5$	$rmGlu_7$	$rmGlu_8$
27o	Inactive					
	Eurofins Lead Profiling					
	Receptor			% Inhibition @ 10 μM		
27o	Adenosine A_3			76		

Finally, since $mGlu_4$ has emerged as a target for the possible treatment of PD, we assessed the efficacy of **27o** (10 mg/kg) in the rat haloperidol-induced catalepsy (HIC) model, (Table 10A).[46] This compound showed robust activity in this model after oral administration (One-way ANOVA: $F_{2,27} = 101.8$, $p < 0.0001$) – comparable to previously evaluated $mGlu_4$ PAMs (**4**, Table 10A) and previously published adenosine A_{2A} antagonists. To better understand *in vivo* efficacy in relation to exposure (PK/PD), we quantified the plasma, brain and cerebrospinal fluid (CSF) levels of **27o**. As shown in Table 10B, the reversal of HIC was observed with total brain levels of 252 nM ($K_p = 0.23$) and CSF levels of 46 nM. We also evaluated **27o** for potential efflux (Table 10) but no significant efflux was noted (MDCK-Pgp ER: 1.9) (Table 10C). These levels of drug vs. efficacy in HIC is similar to other $mGlu_4$ PAMs developed in our laboratory and further supports the use of total brain and CSF levels of drug to correlate PK/PD.

Table 10. *In vivo* evaluation after haloperidol assay.

A

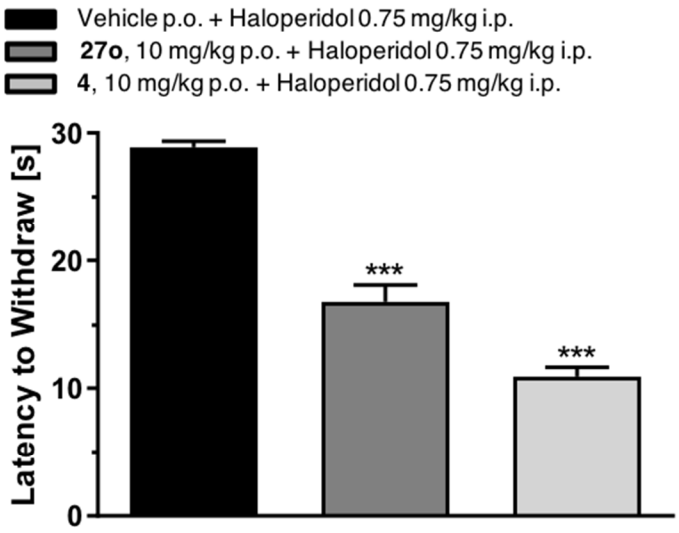

Statistics: **27o**, Reversal of Haloperidol-induced Catalepsy in male Sprague-Dawley rats. One-way ANOVA: $F_{2,27} = 101.8$, $p < 0.0001$. ***$p < 0.0001$ vs. Vehicle + Haloperidol (Dunnett's multiple comparison test). N = 10 animals/group.

B. *In vivo* exposure in rat plasma/brain after PO administration in haloperidol-induced catalepsy

Cmpd	Dose (mg/kg)	Plasma (nM)	Brain (nM)	CSF (nM)
27o	10	1120	252	46.0

C. MDCK-Pgp (P_{app}, 10^{-6} cm/s)

	A-B	B-A	Efflux
27o	2.9	5.4	1.9

CONCLUSION

Herein, we have presented the synthesis and biological characterization of a highly potent and selective $mGlu_4$ PAM benzo[*d*]isothiazole-based scaffold. These compounds were prepared based on previous work from our laboratories with the design aimed at targeting compounds that mitigate the CYP1A2 induction issue but yield metabolically stable compounds that can be evaluated in preclinical models of PD. The lead compound, **27o**, exhibited potent PAM activity against both the human and rat $mGlu_4$ receptors as well as selectivity against the other mGlu receptors and a wider selectivity panel. Studies with the rodent haloperidol-induced catalepsy model confirm that **27o** is active with sufficient brain and CSF levels (PK/PD). In conclusion,

this new scaffold represents a new and improved $mGlu_4$ PAM molecule for further study in additional preclinical models.

EXPERIMENTAL SECTION

Reagents and General Methods. All ^{1}H & ^{13}C NMR spectra were recorded on Bruker AV-400 (400 MHz) or Bruker AV-NMR (600 MHz) instrument. Chemical shifts are reported in ppm relative to residual solvent peaks as an internal standard set to δH 7.26 or δC 77.0 ($CDCl_3$) and δH 3.31 or δC 49.0 (CD_3OD). Data are reported as follows: chemical shift, multiplicity (s =singlet, d = doublet, t = triplet, q = quartet, br = broad, m = multiplet), integration, coupling constant (Hz). IR spectra were recorded as thin films and are reported in wavenumbers (cm-1). Low resolution mass spectra were obtained on an Agilent 1200 LCMS with electrospray ionization. High resolution mass spectra were recorded on a Waters Qtof-API-US plus Acquity system. The value Δ is the error in the measurement (in ppm) given by the equation $\Delta = [(ME - MT)/ MT] \times 106$, where ME is the experimental mass and MT is the theoretical mass. The HRMS results were obtained with ES as the ion source and leucine enkephalin as the reference. Low resolution mass spectra were obtained on an Agilent 1200 LCMS with electrospray ionization, with a gradient of 5-95% MeCN in 0.1% TFA water over 1.5 min. Analytical thin layer chromatography was performed on 250 μM silica gel 60 F254 plates. Visualization was accomplished with UV light, and/or the use of ninhydrin, anisaldehyde and ceric ammonium molybdate solutions followed by charring on a hot-plate. Chromatography on silica gel was performed using Silica Gel 60 (230-400 mesh) from Sorbent Technologies. Solvents for extraction, washing and chromatography were HPLC grade. All reagents were purchased from Aldrich Chemical Co. and were used without purification. Flame-dried (under vacuum) glassware was used for all reactions. All reagents and solvents were commercial grade and

purified prior to use when necessary. Mass spectra were obtained on a Micromass Q-Tof API-US mass spectrometer was used to acquire high-resolution mass spectrometry (HRMS) data. Microwave synthesis was performed on an Initiator+ by Biotage.

Compounds were purified on a Gilson preparative reversed-phase HPLC system comprised of a 333 aqueous pump with solvent-selection valve, 334 organic pump, GX-271 or GX-281 liquid hander, two column switching valves, and a 155 UV detector. UV wavelength for fraction collection was user-defined, with absorbance at 254 nm always monitored. Column: Phenomenex Axia-packed Gemini C18, 30 x 50 mm, 5 μm. For Acidic Method: Mobile phase: CH_3CN in H_2O (0.1% TFA). Gradient conditions: 0.75 min equilibration, followed by user-defined gradient (starting organic percentage, ending organic percentage, duration), hold at 95% CH_3CN in H_2O (0.1% TFA) for 1 min, 50 mL/min, 23° C. For Basic Method: Mobile phase: CH_3CN in H_2O (0.05% v/v NH_4OH). Gradient conditions: 0.75 min equilibration, followed by user-defined gradient (starting organic percentage, ending organic percentage, duration), hold at 95% CH_3CN in H_2O (0.05% v/v NH_4OH) for 1 min, 50 mL/min, 23° C. The purity of all compounds was determined by LCMS to be >95% (or as stated).

General synthetic procedure for (21) or (24). To a solution of 4-bromo-2-fluorobenzaldehyde, **20**, (1 eq.) or 5-bromo-3-fluoropicolinonitrile, **23**, in THF (1 mL) at 0 ^oC was added RMgBr (2 eq.). The reaction was removed from the ice bath and allowed to stir at rt for 24 h. The reaction was neutralized with a solution of NH_4Cl (2 mL) and diluted with EtOAc (10 mL). The organic layers were washed with water (2x20 mL). The aqueous layer was extracted with EtOAc (2x20 mL). Organic layers were combined, and solvent was removed under reduced pressure to yield **21** or **24**. The product yield was assumed to be 100% and was used for further reactions without purification.

1-(4-bromo-2-fluoro-phenyl)-3,3-dimethyl-butan-1-ol (21a). To a solution of 4-bromo-2-fluorobenzaldehyde (1.00 g, 4.93 mmol) in THF (1 mL) at 0 ^{o}C was added chloro(2,2-dimethylpropyl)magnesium (9.91 mL, 9.91 mmol). The reaction was removed from the ice bath and allowed to stir at rt for 24 h. The reaction was neutralized with a solution of NH_4Cl (2 mL) and diluted with EtOAc (10 mL). The organic layers were washed with water (2x20 mL). The aqueous layer was extracted with EtOAc (2x20 mL). Organic layers were combined, and solvent was removed under reduced pressure to yield 1-(4-bromo-2-fluoro-phenyl)-3,3-dimethyl-butan-1-ol, **21a**, as a yellow oil. The product yield was assumed to be quantitative and was used for further reactions without purification.

General synthetic procedure for (22). To a crude suspension of **21** (1 eq.) in DCM (10 mL) at rt was added Dess-Martin periodinane (1 eq.). After 1 h, the reaction was diluted with DCM (10 mL) and washed with a saturated solution of $Na_2S_2O_3$ (25 mL) and $NaHCO_3$ (25 mL). The extract was filtered through a hydrophobic filter and concentrated under reduced pressure to yield **22**. The product yield was assumed to be quantitative and was used for further reactions without purification.

1-(4-bromo-2-fluoro-phenyl)-3,3-dimethyl-butan-1-one (22a). To a crude suspension of **21a** (1.36 mg, 4.92 mmol) in DCM (10 mL) at rt was added Dess-Martin periodinane (2.09 mg, 4.92 mmol). After 1 h, the reaction was diluted with DCM (10 mL) and washed with a saturated solution of $Na_2S_2O_3$ (25 mL) and $NaHCO_3$ (25 mL). The extract was filtered through a hydrophobic filter and concentrated under reduced pressure to yield 1-(4-bromo-2-fluoro-phenyl)-3,3-dimethyl-butan-1-one, **22a**. The product yield was assumed to be quantitative and was used for further reactions without purification. LCMS: R_T = 1.324 min, *m/z* = 273.2 $[M + H]^+$.

General synthetic procedure for (25). A solution of benzyl mercaptan (0.56 mL, 4.8 mmol) in THF (4 mL) was added dropwise to a solution of potassium *tert*-butoxide (534 mg, 4.76 mmol) in THF (20 mL). After 5 min at rt, a solution of **22** or **24** (1 eq.) in THF (5 mL) was added. The reaction was stirred at rt for 30 min and consumption of starting material was followed by LCMS. Upon completion, the reaction mixture was added to a mixture of EtOAc:water (2:1; 150 mL). The organic layer was separated and washed with water (3x150 mL). The aqueous layer was extracted with EtOAc (100 mL). Combined organic layers were dried over $MgSO_4$ and concentrated under reduced pressure. The residue solid was suspended in a solution of 10% EtOAc in hexanes (20 mL) and transferred to a silica gel column. Fractions were manually collected in a 10% EtOAc in hexanes elution from the silica. Fractions were combined concentrated under reduced pressure to yield **25**. Product yield was assumed to be quantitative and was used for further reactions without purification.

1-(2-benzylsulfanyl-4-bromo-phenyl)-3,3-dimethyl-butan-1-one (25a). A solution of benzyl mercaptan (0.56 mL, 4.8 mmol) in THF (4 mL) was added dropwise to a solution of potassium tert-butoxide (534 mg, 4.76 mmol) in THF (20 mL). After 5 min at rt, a solution of 1-(4-bromo-2-fluoro-phenyl)-3,3-dimethyl-butan-1-one **22a** (1.30 g, 4.76 mmol) in THF (5 mL) was added. The reaction was stirred at rt for 30 min and consumption of starting material was followed by LCMS. Upon completion, the reaction mixture was added to a mixture of EtOAc:H_2O (2:1; 150 mL). The organic layer was separated and washed with water (3x150 mL). The aqueous layer was extracted with EtOAc (100 mL). Combined organic layers were dried over $MgSO_4$ and concentrated under reduced pressure. The residue solid was suspended in a solution of 10% EtOAc in hexanes (20 mL) and transferred to a silica gel column. Fractions were manually collected in a 10% EtOAc in hexanes elution from the silica. Fractions were

combined concentrated under reduced pressure to yield 1-(2-benzylsulfanyl-4-bromo-phenyl)-3,3-dimethyl-butan-1-one, **25a**, as a light-brown oil. Product yield was assumed to be 100% and was used for further reactions without purification. LCMS: R_T = 1.454 min, *m/z* = 379.4 $[M + H]^+$.

General synthetic procedure for (26). To a solution of **25** (1 eq.) in DCE (12 mL) was added dropwise a solution of sulfuryl chloride (1 eq.) in DCE (0.5 mL). After 30 min at rt, the reaction was concentrated under reduced pressure. To the residue was added THF (12 mL) and ammonia (7M in MeOH, 3 eq.). After 30 min at rt, to the reaction was added water (5 mL). The reaction was extracted with EtOAc (50 mL) and washed with water (2x100 mL). Organic layer was dried over Na_2SO_4, filtered, and concentrated under reduced pressure. The residue was dissolved in DMSO (10 mL) and purified via reverse phase HPLC (5-95% MeCN/ in water (0.1% TFA). Fractions were combined and concentrated under reduced pressure to yield **26** (28-82% yield).

6-bromo-3-neopentylbenzo[*d*]isothiazole (26a). To a solution of **25a** (1.60 g, 4.23 mmol) in DCE (12 mL) was added dropwise a solution of sulfuryl chloride (0.34 mL, 4.2 mmol) in DCE (0.5 mL). After 30 min at rt, the reaction was concentrated under reduced pressure. To the residue was added THF (12 mL) and ammonia (7 M in MeOH, 2.0 mL, 14 mmol). After 30 min at rt, to the reaction was added water (5 mL). The reaction was extracted with EtOAc (50 mL) and washed with water (2x100 mL). Organic layer was dried over Na_2SO_4, filtered, and concentrated under reduced pressure. The residue was dissolved in DMSO (10 mL) and purified via reverse phase HPLC (5-95% MeCN/0.1% TFA in water). Fractions were combined and concentrated under reduced pressure to yield 6-bromo-3-(2,2-dimethylpropyl)-1,2-benzothiazole,

26a (410 mg, 1.44 mmol, 34.1% yield) as an off-white solid. LCMS: R_T = 1.414 min, purity 90% at 215 and 254nm, *m/z* = 286.0 $[M + H]^+$.

General synthetic procedure for (27a-i). A 2 mL vial was charged with sodium *tert*-butoxide (1.5 eq.), Pd-^{t}BuXPhos (2.0 mol%), ^{t}BuXPhos (2.0 mol%), **9** (1 eq.), and **26** (1 eq.). The reaction was evacuated and purged with Nitrogen (3x). To the vial was added *tert*-butanol (2 mL) and the heterogeneous mixture was heated to 60 ^{o}C for 2 h. The reaction was added to a mixture of EtOAc (10 mL) and water (20 mL). Organic layers were collected and washed with water (20 mL). Aqueous layer was extracted with EtOAc (5x50 mL). Organic extractions were combined, and solvent was removed under reduced pressure. Residue was suspended in TFA (2 mL) and transferred to a 2 mL microwave vial. The reaction was heated to 150 °C for 15 min in a microwave reactor. Solvent was removed under reduced pressure, and residue was dissolved in DMSO (5 mL). The solution was filtered and purified via reverse phase HPLC (5-95% MeCN/0.1%TFA water). Fractions were added to a mixture of EtOAc (50 mL) and water (50 mL) and saturated $NaHCO_3$ (2 mL). Organic layer was separated and washed with water (2x) and brine. Aqueous layer was re-extracted with EtOAc. Solvent was dried over $MgSO_4$, filtered, and concentrated under reduced pressure to yield **27a** (16-52% yield).

3-neopentyl-*N*-(1*H*-pyrazolo[4,3-*b*]pyridin-3-yl)benzo[*d*]isothiazol-6-amine (27a). In a 2 mL vial, was added sodium tert-butoxide (37 mg, 0.38 mmol), Pd-^{t}BuXPhos (3 mg, 0.005 mmol), ^{t}BuXPhos (2 mg, 0.005 mmol), **9** (61 mg, 0.24 mmol), and **26a** (68 mg, 0.24 mmol). The reaction was evacuated and purged with Nitrogen (3x). To the vial was added tert-butanol (2 mL) and the heterogeneous mixture was heated to 60 ^{o}C for 2 h. The reaction was added to a mixture of EtOAc (10 mL) and water (20 mL). Organic layers were collected and washed with water (20 mL). Aqueous layer was extracted with EtOAc (5x50 mL). Organic extractions were

combined, and solvent was removed under reduced pressure. Residue was suspended in TFA (2 mL) and transferred to a 2 mL microwave vial. The reaction was heated to 150 °C for 15 min in a microwave reactor. Solvent was removed under reduced pressure, and residue was dissolved in DMSO (5 mL). The solution was filtered and purified via reverse phase HPLC (5-95% MeCN/0.1%TFA water). Fractions were added to a mixture of EtOAc (50 mL) and water (50 mL) and saturated $NaHCO_3$ (2 mL). Organic layer was separated and washed with water (2x) and brine. Aqueous layer was re-extracted with EtOAc. Solvent was dried over $MgSO_4$, filtered, and concentrated under reduced pressure to yield 3-neopentyl-*N*-(1*H*-pyrazolo[4,3-*b*]pyridin-3-yl)benzo[*d*]isothiazol-6-amine, **27a.** (37.6 mg, 0.111 mmol, 47% yield) as an off-white solid. LCMS: R_T = 1.067 min, purity >98% at 215 and 254 nm, *m/z* = 338.4 $[M + H]^+$. ^1H NMR (400 MHz, DMSO-d_6): δ 9.69 (s, 1 H), 8.63 (d, *J* = 1.8 Hz, 1 H), 8.48 (dd, *J* = 4.3, 1.3 Hz, 1 H), 8.00 (d, *J* = 8.9 Hz, 1 H), 7.93 (dd, *J* = 8.5, 1.2 Hz, 1 H), 7.75 (dd, *J* = 8.9, 1.9 Hz, 1 H), 7.43 (dd, *J* = 8.7, 4.3 Hz, 1 H), 2.94 (s, 2 H), 1.00 (s, 9 H).

3-neopentyl-*N*-(1*H*-pyrazolo[4,3-*b*]pyridin-3-yl)isothiazolo[4,5-*b*]pyridin-6-amine (27b). The compound, **27b**, was synthesized following the procedure outlined in General Scheme 4 (47% yield). LCMS: R_T = 1.050 min, purity >98% at 215 and 254 nm, *m/z* = 339.2 $[M + H]^+$.

3-neopentyl-*N*-(1*H*-pyrazolo[3,4-*b*]pyridin-3-yl)benzo[*d*]isothiazol-6-amine (27c). The compound, **27c**, was synthesized following the procedure outlined in General Scheme 4 (9% yield). LCMS: R_T = 1.074 min, purity >98% @ 215 and 254 nm, *m/z* = 338.4 $[M + H]^+$.

3-neopentyl-*N*-(1*H*-pyrazolo[3,4-*b*]pyrazin-3-yl)isothiazolo[4,5-*b*]pyridin-6-amine (27d). The compound, **27d**, was synthesized following the procedure outlined in General

Scheme 4 (13% yield). LCMS: R_T = 1.050 min, purity >98% @ 215 and 254 nm, *m/z* = 340.2 $[M + H]^+$.

3-ethyl-*N*-(1*H*-pyrazolo[4,3-*b*]pyridin-3-yl)benzo[*d*]isothiazol-6-amine (27e). The compound, **27e**, was synthesized following the procedure outlined in General Scheme 4 (16% yield). LCMS: R_T = 0.808 min, purity >98% @ 215 and 254 nm, *m/z* = 297.2 $[M + H]^+$.

3-ethyl-*N*-(1*H*-pyrazolo[3,4-*b*]pyridin-3-yl)benzo[*d*]isothiazol-6-amine (27f). The compound, **27f**, was synthesized following the procedure outlined in General Scheme 4 (10% yield). LCMS: R_T = 0.820 min, purity >98% @ 215 and 254 nm, *m/z* = 297.2 $[M + H]^+$.

3-cyclopropyl-*N*-(1*H*-pyrazolo[4,3-*b*]pyridin-3-yl)benzo[*d*]isothiazol-6-amine (27g). The compound, **27g**, was synthesized following the procedure outlined in General Scheme 4 (45% yield). LCMS: R_T = 0.919 min, purity >98% @ 215 and 254 nm, *m/z* = 308.3 $[M + H]^+$.

3-cyclopropyl-*N*-(1*H*-pyrazolo[3,4-*b*]pyrazin-3-yl)benzo[*d*]isothiazol-6-amine (27h). The compound, **27h**, was synthesized following the procedure outlined in General Scheme 4 (35% yield). LCMS: R_T = 0.943 min, purity >98% @ 215 and 254 nm, *m/z* = 309.4 $[M + H]^+$.

3-(*tert*-butyl)-*N*-(1*H*-pyrazolo[4,3-*b*]pyridin-3-yl)benzo[*d*]isothiazol-6-amine (27i). The compound, **27i**, was synthesized following the procedure outlined in General Scheme 4 (28% yield). LCMS: R_T = 1.033 min, purity >98% @ 215 and 254 nm, *m/z* = 324.4 $[M + H]^+$.

***N*-(1*H*-pyrazolo[3,4-*b*]pyridin-3-yl)-3-(trifluoromethyl)benzo[*d*]isothiazol-6-amine (27j).** In a 2 mL vial, was added sodium *tert*-butoxide (21 mg, 0.22 mmol), Pd-^{t}BuXPhos (2 mg, 0.003 mmol), ^{t}BuXPhos (1 mg, 0.003 mmol), **9** (35 mg, 0.14 mmol), and **30** (38 mg, 0.14 mmol). The reaction was evacuated and purged with Nitrogen (3x). To the vial was added *tert*-butanol (2 mL) and the heterogeneous mixture was heated to 75 ^{o}C for 1 h. The reaction was added to a mixture of EtOAc (10 mL) and water (20 mL). Organic layers were collected and

washed with water (20 mL). Aqueous layer was extracted with EtOAc (5x50 mL). Organic extractions were combined, and solvent was removed under reduced pressure. Residue was suspended in TFA (2 mL) and transferred to a 2 mL microwave vial. The reaction was heated to 150 °C for 15 min in a microwave reactor. Solvent was removed under reduced pressure, and residue was dissolved in DMSO (2 mL). The solution was filtered and purified via reverse phase HPLC (5-95% MeCN/0.1%TFA water). Fractions were added to a mixture of EtOAc (50 mL) and water (50 mL) and saturated aqueous $NaHCO_3$ (2 mL). The separated organic layer was washed with water (2x) and brine. Aqueous layer was re-extracted with EtOAc. Solvent was dried over $MgSO_4$, filtered, and concentrated under reduced pressure to yield *N*-(1*H*-pyrazolo[3,4-*b*]pyridin-3-yl)-3-(trifluoromethyl)benzo[*d*]isothiazol-6-amine, **27j** (13.4 mg, 29% yield over 2 steps). LCMS: R_T = 1.024 min, purity >98% @ 215 and 254 nm, *m/z* = 336.2 $[M + H]^+$.

2-(6-((1*H*-pyrazolo[4,3-*b*]pyridin-3-yl)amino)benzo[*d*]isothiazol-3-yl)propan-2-ol (27k). To a solution of **33** (84 mg, 0.27 mmol, 1 eq) in THF (0.1 M) at -78 °C was added dropwise methylmagnesium bromide (0.45 mL, 3 M in diethyl ether). After 1 h at -78 °C, the cold bath was replaced with an ice bath. After 1 h at 0 °C, a saturated solution of NH_4Cl (5 mL) was added and the reaction mixture was extracted with $CHCl_3$:IPA (2x50 mL). The combined extracts were washed with brine, dried ($MgSO_4$), filtered and concentrated under reduced pressure. The residue was dissolved in DMSO and purified by reversed phase HPLC (15-55% acetonitrile/water with 0.1% TFA). The fractions were concentrated to afford desired product, **27k**, (13% yield). LCMS: R_T = 0.761 min, purity >98% at 215 and 254 nm, *m/z* = 326.2 $[M + H]^+$.

1-(4-(6-((1*H*-pyrazolo[4,3-*b*]pyridin-3-yl)amino)benzo[*d*]isothiazol-3-yl)piperidin-1-yl)ethan-1-one (27l). In a 2 mL vial, was added sodium *tert*-butoxide (136 mg, 1.41 mmol), Pd-^{t}BuXPhos (12 mg, 0.017 mmol), ^{t}BuXPhos (8 mg, 0.017 mmol), **9** (224 mg, 0.88 mmol), and **42** (300 mg, 0.88 mmol). The reaction was evacuated and purged with Nitrogen (3x). To the vial was added *tert*-butanol (10 mL) and the heterogeneous mixture was heated to 75 ^{o}C for 2 h. To the reaction was added and water (50 mL) and extracted with IPA:$CHCl_3$ (1:3; 5x50 mL). Organic layers were collected and the solvent was removed under reduced pressure. Residue was suspended in TFA (2 mL) and transferred to a 2 mL microwave vial. The reaction was heated to 150 °C for 15 min in microwave reactor. Solvent was removed under reduced pressure, and residue was dissolved in DMSO (5 mL). The solution was filtered and purified via reverse phase HPLC (5-95% MeCN/0.1%TFA water). Fractions were added to a mixture of EtOAc (50 mL) and water (50 mL) and saturated $NaHCO_3$ (2 mL). Organic layer was separated and washed with water (2x25 mL) and brine (25 mL). Aqueous layer was extracted with EtOAc. Solvent was dried ($MgSO_4$), filtered, and concentrated under reduced pressure to yield 3-(2,2-dimethylpropyl)-*N*-(1*H*-pyrazolo[4,3-*b*]pyridin-3-yl)-1,2-benzothiazol-6-amine, **27a.** (311 mg, 69% yield). LCMS: R_T = 0.784 min, purity >98% at 215 and 254 nm, *m/z* = 393.3 $[M + H]^+$. ^{1}H NMR (400 MHz, $CDCl_3$): δ 9.51 (br s, 1 H), 8.68 (d, *J* = 1.8 Hz, 1 H), 8.54 (d, *J* = 4.5 Hz, 1 H), 7.91-7.88 (m, 2 H), 7.48-7.44 (m, 2 H), 4.74-4.71 (m, 1 H), 4.08-4.02 (m, 1 H), 3.53-3.43 (m, 1 H), 3.37-3.26 (m, 1 H), 2.95-2.88 (m, 1 H), 2.19 (s, 3 H), 2.16-2.08 (m, 3 H), 2.00-1.90 (m, 1 H). HRMS: Calculated for $C_{20}H_{20}N_6OS$, 392.1419; found, 392.1423.

(4-(6-((1*H*-pyrazolo[4,3-*b*]pyridin-3-yl)amino)benzo[*d*]isothiazol-3-yl)piperidin-1-yl)(cyclopropyl)methanone (27m). The compound, **27m**, was synthesized following the procedure

outlined in General Scheme 7. LCMS: R_T = 0.881 min, purity >98% @ 215 and 254 nm, *m/z* = 419.3 $[M + H]^+$.

General synthetic procedure for (27n-v). To a mixture of **34** (1 eq), HATU (1.5 eq) and amine (2 eq) in DMF (0.2 M) at rt was added DIEA (4 eq). The reaction was monitored by LCMS. Upon completion, the reaction mixture was purified by reversed phase Gilson HPLC (60-90% acetonitrile/water with 0.1% TFA). After concentration of the solvent, the residue was dissolved in TFA (0.1 M) and the solution was heated in the microwave for 30 min at 150 °C. Solvent was removed and the residue was dissolved in DMSO and purified by reversed phase Gilson HPLC (30-60% acetonitrile/water with 0.1% TFA) to yield the desired products.

(6-((1*H*-pyrazolo[4,3-*b*]pyridin-3-yl)amino)benzo[*d*]isothiazol-3-yl)(3,3-difluoropyrrolidin-1-yl)methanone (27n). The compound, **27n**, was synthesized following the procedure outlined in General Scheme 8 (15% yield). LCMS: R_T = 0.864 min, purity >98% @ 215 and 254 nm, *m/z* = 401.0 $[M + H]^+$.

6-((1*H*-pyrazolo[4,3-*b*]pyridin-3-yl)amino)-N-(3,3-difluorocyclobutyl)benzo[*d*]isothiazole-3-carboxamide (27o). The compound, **27o**, was synthesized following the procedure outlined in General Scheme 8 (55% yield). LCMS: R_T = 0.927 min, purity >98% at 215 and 254 nm, *m/z* = 401.0 $[M + H]^+$. ^{1}H NMR (400 MHz, DMSO-d_6): δ 9.91 (s, 1 H), 9.29 (d, *J* = 7.2 Hz, 1 H), 8.70 (d, *J* = 1.8 Hz, 1 H), 8.55-8.52 (m, 2 H), 8.01 (d, *J* = 8.5 Hz, 1 H), 7.79 (dd, *J* = 9.0, 1.9 Hz, 1 H), 7.48 (dd, *J* = 8.5, 4.3 Hz, 1 H), 4.39-4.30 (m, 1 H), 3.00-2.83 (m, 4 H). HRMS: Calculated for $C_{18}H_{14}F_2N_6OS$, 400.0918; found, 400.0918.

6-((1*H*-pyrazolo[3,4-*b*]pyrazin-3-yl)amino)-*N*-(3,3-difluorocyclobutyl)benzo[*d*]isothiazole-3-carboxamide (27p). The compound, **27p**, was

synthesized following the procedure outlined in General Scheme 8 (21% yield). LCMS: R_T = 0.946 min, purity >98% @ 215 and 254 nm, *m/z* = 402.2 $[M + H]^+$.

6-((1*H*-pyrazolo[4,3-*b*]pyridin-3-yl)amino)-*N*-(3,3-difluorocyclobutyl)-*N*-methylbenzo[*d*]iso-thiazole-3-carboxamide (27q). The compound, **27q**, was synthesized following the procedure outlined in General Scheme 8 (18% yield). LCMS: R_T = 0.892 min, purity >98% @ 215 and 254 nm, *m/z* = 415.2 $[M + H]^+$.

(6-((1*H*-pyrazolo[4,3-*b*]pyridin-3-yl)amino)benzo[*d*]isothiazol-3-yl)(4,4-difluoropiperidin-1-yl)methanone (27r). The compound, **27r**, was synthesized following the procedure outlined in General Scheme 8 (13% yield). LCMS: R_T = 0.837 min, purity >98% @ 215 and 254 nm, *m/z* = 415.0 $[M + H]^+$.

(6-((1*H*-pyrazolo[4,3-*b*]pyridin-3-yl)amino)benzo[*d*]isothiazol-3-yl)(morpholino)methanone (27s). The compound, **27s**, was synthesized following the procedure outlined in General Scheme 8 (11% yield). LCMS: R_T = 0.681 min, purity >98% @ 215 and 254 nm, *m/z* = 381.2 $[M + H]^+$.

(6-((1*H*-pyrazolo[4,3-*b*]pyridin-3-yl)amino)benzo[*d*]isothiazol-3-yl)(2,6-dimethyl morpholino)methanone (27t). The compound, **27t**, was synthesized following the procedure outlined in General Scheme 8 (13% yield). LCMS: R_T = 0.814 min, purity >98% @ 215 and 254 nm, *m/z* = 409.2 $[M + H]^+$.

(6-((1*H*-pyrazolo[4,3-*b*]pyridin-3-yl)amino)benzo[*d*]isothiazol-3-yl)(3,5-dimethylpiperidin-1-yl)methanone (27u). The compound, **27u**, was synthesized following the procedure outlined in General Scheme 8 (4% yield). LCMS: R_T = 1.026 min, purity >98% @ 215 and 254 nm, *m/z* = 407.2 $[M + H]^+$.

(6-((1*H*-pyrazolo[4,3-*b*]pyridin-3-yl)amino)benzo[*d*]isothiazol-3-yl)(4-methylpiperidin-1-yl) methanone (27v). The compound, **27v**, was synthesized following the procedure outlined in General Scheme 8 (16% yield). LCMS: R_T = 0.962 min, purity >98% @ 215 and 254 nm, *m/z* = 393.2 $[M + H]^+$.

3-((4,4-difluoropiperidin-1-yl)methyl)-*N*-(1*H*-pyrazolo[4,3-*b*]pyridin-3-yl)isothiazolo[4,5-*b*]pyridin-6-amine (27w). In a 2 mL vial, was added sodium *tert*-butoxide (13 mg, 0.14 mmol), Pd-^{t}BuXPhos (1.2 mg, 0.002 mmol), ^{t}BuXPhos (0.7 mg, 0.002 mmol), **9** (22 mg, 0.09 mmol), and **37** (30 mg, 0.09 mmol). The reaction was evacuated and purged with Nitrogen (3x). To the vial was added *tert*-butanol (2 mL) and the heterogeneous mixture was heated to 75 ^oC for 1 h. The reaction was added to a mixture of EtOAc (20 mL) and water (20 mL). Organic layers were collected and washed with water (2x50 mL). Aqueous layer was extracted with EtOAc (20 mL). The combined organic layers were concentrated under reduced pressure. The residue was suspended in TFA (2 mL) and heated to 150 °C for 20 min in a microwave reactor . Solvent was removed under reduced pressure, and residue was dissolved in DMSO (2 mL). The solution was filtered and purified via reverse phase HPLC (5-95% MeCN/0.05% NH_4OH in water) to afford 3-((4,4-difluoropiperidin-1-yl)methyl)-*N*-(1*H*-pyrazolo[4,3-*b*]pyridin-3-yl)isothiazolo[4,5-*b*]pyridin-6-amine, **27w** (15 mg, 43% yield over 2 steps). LCMS: R_T = 0.660 min, purity >98% @ 215 and 254 nm, *m/z* = 402.2 $[M + H]^+$.

2-(benzylthio)-4-bromobenzaldehyde (28). Benzyl mercaptan (0.58 mL, 4.9 mmol) in THF (4 mL) was added dropwise to a solution of sodium tert-butoxide (0.56 g, 5.8 mmol) in THF (20 mL). After 5 min at rt, a solution of 4-bromo-2-fluorobenzaldehyde (1.0 g, 4.9 mmol) in THF (5 mL) was added. The reaction was monitored via LCMS. The reaction was added to EtOAc/water (1:1; 100 mL). The organic layer was washed with water (3x30 mL), dried

(Na_2SO_4), filtered and concentrated. The residue was purified on normal phase chromatography (0-25% EtOAc/hexanes) to afford desired product (0.56 g, 37% yield). LCMS: R_T = 1.239 min, purity >98% @ 215 and 254 nm, *m/z* = 307.0 $[M + H]^+$.

1-(2-(benzylthio)-4-bromophenyl)-2,2,2-trifluoroethan-1-one (29). To a solution of 2-(benzylthio)-4-bromobenzaldehyde, **28**, (0.56 g, 1.81 mmol) in THF (50 mL) at 0 °C was added trimethyl(trifluoromethyl)silane (0.35 mL, 2.17 mmol) dropwise over 5 min. After 15 min at 0 °C, to the reaction was added TBAF (0.18 mL, 0.18 mmol) dropwise. The ice bath was removed and after 16 hours at rt, the reaction was cooled to 0 °C. To the reaction was added 3M HCl (aq) (12 mL). The ice bath was removed and after 16 hours at rt, the reaction was added to EtOAc (100 mL). The organic layer was separated and washed with water (2x25 mL), brine (25 mL) and dried (Na_2SO_4). After filtration, the solution was concentrated and purified by normal phase chromatography (5-35% EtOAc/hexanes) to provide 1-(2-(benzylthio)-4-bromophenyl)-2,2,2-trifluoroethan-1-ol (0.68 g, 99% yield).

To a suspension of 1-(2-(benzylthio)-4-bromophenyl)-2,2,2-trifluoroethan-1-ol (0.68 g, 1.8 mmol) in DCM (10 mL) at rt was added Dess-Martin periodinane (1.0g, 2.36 mmol). After 1 h, the reaction was diluted with DCM and washed with 10% NaS_2O_3 (aq), followed by $NaHCO_3$ (sat'd aqueous). The organic layer was filtered through a hydrophobic filter and concentrated under reduced pressure to yield 1-(2-(benzylthio)-4-bromophenyl)-2,2,2-trifluoroethan-1-one. Product was carried forward without further purification.

6-bromo-3-(trifluoromethyl)benzo[*d*]isothiazole (30). To a solution of 1-(2-(benzylthio)-4-bromophenyl)-2,2,2-trifluoroethan-1-one (1.8 g, 4.9 mmol) in DCE (12 mL) was added dropwise a solution of sulfuryl chloride (0.67 g, 4.9 mmol) in DCE (1 mL). After 30 min at rt, the reaction was concentrated under reduced pressure. To the residue was added THF (12

mL) followed by ammonia (1 mL, 7M in MeOH) dropwise. Immediately, a white precipitate was formed. After 16 hours at rt, water (10 mL) was added to the reaction mixture. The reaction was extracted with EtOAc (25 mL) and the organic layer was washed with water (2x25 mL), dried (Na_2SO_4), filtered and concentrated. The residue was dissolved in DMSO (5 mL) and purified via reverse phase HPLC (5-95% MeCN/0.1%TFA water). The desired fractions were combined and concentrated to yield 6-bromo-3-(trifluoromethyl)benzo[d]isothiazole (40 mg, 4% yield over 3 steps). ^{1}H NMR (400 MHz, $CDCl_3$): δ 8.19 (s, 1 H), 8.04 (d, J = 9.1 Hz, 1 H), 7.67 (d, J = 8.8 Hz, 1 H).

Ethyl 6-((1-(4-methoxybenzyl)-1*H*-pyrazolo[4,3-*b*]pyridin-3-yl)amino)benzo[*d*]isothiazole-3-carboxylate (32). In a microwave vial was added ethyl 6-bromobenzo[*d*]isothiazole-3-carboxylate, **31**, (1.0 eq), $Pd_2(dba)_3$ (0.18 eq), Xantphos (0.24 eq), cesium carbonate (2.1 eq) and **9** (1.0 eq). The mixture was evacuated and purged with Nitrogen (3x), followed by the addition of 1,4-dioxane (0.1 M). The reaction mixture was heated to 140 °C for 1 h in a microwave reactor. After confirmation of product via LCMS, the mixture was filtered through a pad of Celite and washed with EtOAc. After the solvent was removed, the crude residue was purified by reversed phase HPLC (60-90% acetonitrile/water with 0.1% TFA). The collected fractions were neutralized with sat. soln. $NaHCO_3$ (aq) and extracted with EtOAc (3x). The combined extracts were washed with brine, dried ($MgSO_4$), filtered and concentrated under reduced pressure to afford ethyl 6-((1-(4-methoxybenzyl)-1*H*-pyrazolo[4,3-*b*]pyridin-3-yl)amino)benzo[*d*]isothiazole-3-carboxylate **32**, (42-46% yield). LCMS: R_T = 1.095 min, purity >98% @ 215 and 254 nM, m/z = 460.2 $[M + H]^+$.

1-(6-((1-(4-methoxybenzyl)-1*H*-pyrazolo[4,3-*b*]pyridin-3-yl)amino)benzo[*d*]isothiazol-3-yl)ethan-1-one (33). To a solution of **32** (300 mg, 0.65 mmol, 1

eq) in THF (0.3 M) at -78 °C was added dropwise methylmagnesium bromide (1.1 mL, 3 M in diethyl ether). After 1.5 h at -78 °C, a saturated solution of NH_4Cl (5 mL) was added. The cold bath was removed and the reaction mixture was extracted with EtOAc (3x50 mL). The combined extracts were washed with brine, dried ($MgSO_4$), filtered and concentrated under reduced pressure. Material was carried forward without further purification. LCMS: R_T = 1.244 min, purity >98% at 215 and 254 nm, *m/z* = 430.3 $[M + H]^+$.

To a mixture of the above product (116 mg, 0.27 mmol, 1 eq) in toluene (0.27 M) was added TFA (1.5 mL). The resulting mixture was heated in the microwave for 30 min at 150 °C. Solvent was removed and the residue was dissolved in DMSO and purified by reversed phase HPLC (15-65% acetonitrile/ 0.1% TFA in water). The fractions were concentrated to afford desired product, **33** (69% yield). LCMS: R_T = 0.897 min, purity >98% at 215 and 254 nm, *m/z* = 310.2 $[M + H]^+$.

6-((1-(4-methoxybenzyl)-1*H*-pyrazolo[4,3-*b*]pyridin-3-yl)amino)benzo[*d*]isothiazole-3-carboxylic acid (34). To a solution of **32** in 1,4-dioxane (0.05 M) and MeOH (0.01 M) was added LiOH (1 N, 5 eq) at rt. The reaction was heated to 40 °C and monitored by LCMS. After complete consumption of the starting material, solvent was removed. The mixture was diluted with water and 1M HCl was added until pH = 2-3 was achieved. The mixture was extracted with $CHCl_3$/IPA (3:1, v/v, 3x). The combined red extracts were washed with brine, dried ($MgSO_4$), filtered and concentrated under reduced pressure. The material was taken through without any further purification. LCMS: R_T = 0.959 min, purity >98% @ 215 and 254 nM, *m/z* = 432.0 $[M + H]^+$.

6-bromo-3-methylisothiazolo[4,5-*b*]pyridine (35). The compound, **35**, was synthesized following the procedure outlined in General Scheme 4.

6-bromo-3-(bromomethyl)isothiazolo[4,5-*b*]pyridine (36). To a solution of 6-bromo-3-methylisothiazolo[4,5-*b*]pyridine (1.3 g, 5.65 mmol) in CCl_4 (15 mL) was added NBS (1.08 g, 6.05 mmol), followed by benzoyl peroxide (0.11 g, 0.45 mmol). The reaction was heated to reflux. After 16 h, the heat was removed. Upon achieving rt, the solution was filtered through a plug of Celite and concentrated under reduced pressure. The material was taken forward without further purification.

6-bromo-3-((4,4-difluoropiperidin-1-yl)methyl)isothiazolo[4,5-*b*]pyridine (37). A solution of 4,4-difluorpiperidine (94 mg, 0.78 mmol) and 6-bromo-3-(bromomethyl)isothiazolo[4,5-*b*]pyridine (200 mg, 0.65 mmol) in NMP (1 mL) was heated to 150 °C in a microwave reactor for 30 min. To the reaction was added DMSO (1 mL) and the mixture was filtered. The DMSO solution was purified via reverse phase HPLC (15-50% MeCN/0.1% TFA in water). The desired fractions were added to EtOAc:water (1:1; 10 mL) with 1 mL of sat. soln. $NaHCO_3$. The organic layer was separated and washed with water (4 mL). After the solvent was removed under reduced pressure, 6-bromo-3-((4,4-difluoropiperidin-1-yl)methyl)isothiazolo[4,5-*b*]pyridine was obtained (61 mg, 27% yield over 2 steps). LCMS: R_T = 0.680 min, purity >98% @ 215 and 254 nm, *m/z* = 350.2 $[M + H]^+$.

1-(4-(4-bromo-2-fluorobenzoyl)piperidin-1-yl)ethan-1-one (40). To 1-bromo-3-fluorobenzene, **38**, (11.5 g, 65.6 mmol) was added $AlCl_3$ (13.1 g, 98.4 mmol) portion-wise over 5 min period. The mixture was heated to 60 °C. After 30 min, 1-acetylpiperidine-4-carbonyl chloride, **39**, (10 g, 52.7 mmol) was added in small portions over 30 min. The reaction mixture was heated to 80 °C for 2 h and then cooled to 60 °C. To the reaction mixture was added chloroform (120 mL) and the slurry was poured onto ice water. The layers were separated and the aqueous layer was extracted with chloroform (3x50 mL). The collected organic layers were

washed with water (2x25 mL), 10% NaOH solution (2 x 25 mL), water (2 x 25 mL). The solvent was removed and the crude residue was dissolved in DMSO (10 mL) and purified via reverse phase HPLC (40-60% MeCN/0.1%TFA water) to afford the desired product (3.6 g, 21% yield).[50]

1-(4-(2-(benzylthio)-4-bromobenzoyl)piperidin-1-yl)ethan-1-one (41). A solution of benzyl mercaptan (1.26 mL, 10.7 mmol) in THF (20 mL) was added dropwise to a solution of potassium tert-butoxide (1.2 g, 12.6 mmol) in THF (60 mL). After 5 min at rt, a solution of 1-(4-(4-bromo-2-fluorobenzoyl)piperidin-1-yl)ethan-1-one **40** (3.52 g, 10.7 mmol) in THF (5 mL) was added. The reaction was stirred at rt for 30 min and consumption of starting material was followed by LCMS. Upon completion, the reaction mixture was added to a mixture of EtOAc:H_2O (2:1; 150 mL). The organic layer was separated and washed with water (3x150 mL). The aqueous layer was extracted with EtOAc (100 mL). Combined organic layers were dried ($MgSO_4$) and concentrated under reduced pressure. Product yield was assumed to be 100% and was used for further reactions without purification.

1-(4-(6-bromobenzo[*d*]isothiazol-3-yl)piperidin-1-yl)ethan-1-one (42). To a solution of 1-(4-(2-(benzylthio)-4-bromobenzoyl)piperidin-1-yl)ethan-1-one (4.6 g, 10.7 mmol) in DCE (40 mL) was added dropwise a solution of sulfuryl chloride (0.96 mL, 11.8 mmol) in DCE (1 mL). After 30 min at rt, the reaction was concentrated under reduced pressure. To the residue was added THF (40 mL) followed by ammonia (7 mL, 7M in MeOH) dropwise. Immediately, a white precipitate was formed. After 1 h at rt, water (10 mL) was added to the reaction mixture. The reaction was extracted with EtOAc (50 mL) and the organic layer was washed with water (2x50 mL), dried (Na_2SO_4), filtered and concentrated. The residue was dissolved in DMSO (5 mL), filtered and purified via reverse phase HPLC (5-95% MeCN/0.1%TFA water). The desired fractions were combined and added to a mixture of EtOAc:water (1:1; 100 mL) and saturated

$NaHCO_3$ (aq) solution. The organic layer was sperated and washed with water (3x20 mL). The aqueous layer was extracted with a mixture of IPA:$CHCl_3$ (1:3; 5x20 mL). The combined organic layers were concentrated to yield 1-(4-(6-bromobenzo[*d*]isothiazol-3-yl)piperidin-1-yl)ethan-1-one (2.0 g, 55% yield over 3 steps).

***In vitro* Pharmacology and Selectivity Assays.** The *in vitro* pharmacology methods and mGlu selectivity assays were performed as previously described.[39, 40] For SAR determination, calcium mobilization $mGlu_4$ assays were performed n = 1 independent times in triplicate. For compounds progressed to *in vivo* studies, experiments were performed 3-6 independent times in either duplicate or triplicate. The maximal response of each compound was determined by normalizing the maximal curve fit response versus that of a standard compound, PHCCC (100% Glu Max). Briefly, Chinese Hamster Ovary (CHO) cells expressing human $mGlu_4$ and the promiscuous G protein G_{qi5} were grown in 90% Dulbecco's Modified Eagle Media (DMEM), 10% dialyzed fetal bovine serum (FBS), 100 units/mL penicillin/streptomycin, 20 mM HEPES (pH 7.3), 1 mM sodium pyruvate, 20 μg/mL proline, 2 mM glutamine, 400 μg/mL G418 sulfate (Mediatech, Inc., Herndon, VA) and 5 nM methotrexate (Calbiochem, EMD Chemicals, Gibbstown, NJ). Cell culture reagents were purchased from Life Technologies (Carlsbad, CA) unless otherwise noted. For the primary calcium mobilization assay, 30,000 cells/20 μL/well were plated in black-walled, clear-bottomed, TC treated, 384 well plates (Greiner Bio-One, Monroe, North Carolina) in DMEM containing 10% dialyzed FBS, 20 mM HEPES, 100 units/mL penicillin/streptomycin, and 1 mM sodium pyruvate (Plating Medium). The cells were grown overnight at 37 °C in the presence of 5% CO_2. The next day, the medium was removed and replaced with 20 μL of 1 μM Fluo-4, AM (Invitrogen, Carlsbad, CA) prepared as a 2.3 mM stock in DMSO and mixed in a 1:1 ratio with 10% (w/v) pluronic acid F-127 and diluted in

Assay Buffer (Hank's balanced salt solution, 20 mM HEPES and 2.5 mM Probenecid (Sigma-Aldrich, St. Louis, MO)) for 45 minutes at 37 °C. Dye was removed and replaced with 20 μL of Assay Buffer. For concentration-response curve experiments, compounds were serially diluted 1:3 into 10-point concentration response curves in DMSO, transferred to daughter plates using an Echo acoustic plate reformatter (Labcyte, Sunnyvale, CA) and diluted in Assay Buffer to a 2X final concentration. Ca^{2+} flux was measured using a Functional Drug Screening System 6000 or 7000 (FDSS6000/7000, Hamamatsu, Japan). After establishment of a fluorescence baseline for 2 seconds (2 images at 1 Hz; excitation, 470 ± 20 nm; emission, 540 ± 30 nm), 20 μL of test compounds was added to the cells, and the response was measured. 142 seconds later, 10 μL (5X) of an EC_{20} concentration of glutamate was added to the cells, and the response of the cells was measured. 147 seconds after this add, an EC_{80} concentration of glutamate was added. Calcium fluorescence was recorded as fold over basal fluorescence and raw data were normalized to the maximal response to glutamate. Potency (EC_{50}) and maximum response (% Glu Max) for compounds were determined for the EC_{20} window using a four parameter logistical equation in Excel (Microsoft Corp, Redmond, WA).

Primary rat $mGlu_4$ thallium flux assay. Potency determinations at rat $mGlu_4$ were performed using a thallium flux assay. Rat $mGlu_4$ was co-expressed with GIRK 1/2 channels in a Human Embryonic Kidney (HEK) cell background. For dye loading, media was exchanged with Assay Buffer (Hanks Balanced Salt Solution (HBSS) containing 20mM HEPES, pH 7.4) using an ELX405 microplate washer (BioTek), leaving 20 μL/well, followed by addition of 20 μL/well 2× FluoZin-2 AM (330 nM final) indicator dye (Life Technologies, prepared as a DMSO stock and mixed in a 1:1 ratio with pluronic acid F-127) in Assay Buffer. After a 1 h incubation at room temperature, dye was exchanged with Assay Buffer, leaving 20 μL/well. Thallium flux was

measured at room temperature using a Functional Drug Screening System 6000 or 7000. Baseline readings were taken (2 images at 1 Hz; excitation, 470 ± 20 nm; emission, 540 ± 30 nm), and test compounds (2×) were added in a 20 μL volume and incubated for 140 s before the addition of 10 μL of Thallium Buffer with or without agonist (5×). Data were collected for an additional 2.5 min and the concentration-response curves were fitted to a four-parameter logistic equation in Excel (Microsoft Corp, Redmond, WA) to determine potency estimates.

mGlu receptor selectivity assays. Activity at human $mGlu_1$ and rat $mGlu_5$ were assessed using calcium mobilization and measuring the glutamate concentration-response relationship in the presence and absence of 10 μM test compound. Using a double-addition protocol, a 10 μM concentration of test compound was added to the cells, followed 2.5 min later by a full concentration range of glutamate. Shifts of the concentration-response relationship were used to assess potential potentiator (left shift of more than 2-fold) or antagonist (right shift of more than 2-fold or depression of the maximum response by at least 75%) activity.

Compound activity at the rat group II and III mGlus was assessed by using thallium flux through GIRKs. HEK cells expressing GIRK1/2 and either $mGlu_2$, $mGlu_3$, $mGlu_7$, or $mGlu_8$ were plated at a density of 15,000 cells/20 μl/well in assay media. Compound activity was assessed by measuring the agonist concentration-response relationship in the presence and absence of 10 μM compound. Using a double-addition protocol, compound was added to the cells, followed 2.5 min later by a full concentration-response of glutamate or, in the case of $mGlu_7$, (2*S*)-2-amino-4-phosphonobutanoic acid. As above, shifts of the concentration-response relationship were used to assess potential potentiator (left shift of more than 2-fold) or antagonist (right shift of more than 2-fold or depression of the maximum response by at least 75%) activity.

***In vitro and in vivo* DMPK Assays.** The *in vitro* and *in vivo* DMPK assays have already been published.[39, 40] All animal studies were approved by the Vanderbilt University Medical Center Institutional Animal Care and Use Committee. The animal care and use program is fully accredited by the Association for Assessment and Accreditation of Laboratory Animal Care, International. For pharmacokinetic and tissue distribution studies via cassette, male Sprague-Dawley rats (n = 1 per experiment) weighing around 300g were purchased from Harlon laboratories (Indianapolis, IN) and implanted with catheters in the carotid artery and jugular vein.[44] The cannulated animals were acclimated to their surroundings for approximately one week before dosing and provided food and water *ad libitum*.

ASSOCIATED CONTENT

Supporting Information

The supporting information is available free of charge on the…

Chemical synthesis and characterization of all analogs, *in vitro* pharmacology/selectivity protocols, *in vitro/in vivo* DMPK protocols and *in vivo* behavior protocols (PDF).

SMILES strings (CSV)

AUTHOR INFORMATION

Corresponding Author

*Department of Pharmaceutical Sciences, Center for Drug Discovery, College of Pharmacy, University of Nebraska Medical Center, 986125 Nebraska Medical Center, Omaha, NE 68198-6125. Phone: 402-559-9729. Fax: 402-559-5643. E-mail: corey.hopkins@unmc.edu

Author Contributions

C.R.H. and C.W.L. oversaw and designed the chemistry. D.W.E., J.D.P., S.R.B., M.W. and J.L.E. performed the synthetic chemistry work. A.L.B. designed the pharmacokinetic

experiments. P.J.C. and C.M.N. designed the *in vitro* pharmacology experiments and M.T.L. and A.L.R. performed the pharmacology experiments. C.K.J. designed the *in vivo* experiments and A.D.T. performed the experiments. C.R.H. wrote the manuscript with input from all authors.

Funding

The authors would also like to thank the Michael J. Fox Foundation for Parkinson's Research for their support of the program to develop $mGlu_4$ PAMs. We also thank William K. Warren, Jr. and the William K. Warren Foundation who funded the William K. Warren, Jr. Chair in Medicine (to C.W.L.).

Notes

The authors declare the following competing financial interest(s): D.W.E., A.L.B., C.K.J., P.J.C., C.W.L., C.M.N., and C.R.H. have received funding and royalties from Bristol-Myers Squibb.

ACKNOWLEDGMENTS

The authors would like to thank Shan Liang, Rocio Zamorano and Daryl Venable for technical assistance with the *in vitro* pharmacology assays, Sichen Cheng for technical assistance with the *in vitro* PK assays and Frank Byers for technical assistance with the *in vivo* PK assays.

ABBREVIATIONS

PD, Parkinson's Disease; mGlu, metabotropic glutamate receptor; BG, basal ganglia; GABA, g-aminobutyric acid; L-DOPA, L-dihydroxyphenylalanine; PAM, positive allosteric modulator; TFA, trifluoroacetic acid; EC_{50}, half maximal effective concentration; MRT, mean residence time; NCS, N-chlorosuccinimide; THF, tetrahydrofuran; PMB, *para*-methoxybenzyl; mW, microwave; DAST, diethylaminosulfur trifluoride; DMPK, drug metabolism and pharmacokinetics; CNS, central nervous system; DMP, Dess-Martin periodinane; TBAF,

tetrabutyammonium fluoride; MeOH, methyl alcohol; DMSO, dimethyl sulfoxide; HATU, 1-[Bis(dimethylamino)methylene]-1*H*-1,2,3-triazolo[4,5-*b*]pyridinium 3-oxide hexafluorophosphate; DIEA, diisopropylethylamine; DMF, *N,N*-dimethylformamide; NMP, N-methylpyrrolidone; EtOAc, ethyl acetate; DCM, dichloromethane; DCE, dichloroethane; LCMS, liquid chromatography-mass spectrometry; HPLC, high performance liquid chromatography; NMR, nuclear magnetic resonance; MeCN, acetonitrile; rt, room temperature; LiOH, lithium hydroxide

REFERENCES

(1) Kalia, L. V., Lang, A. E. Parkinson's disease. *Lancet* **2015**, *386*, 896-912.

(2) https://report.nih.gov/NIHfactsheets/ViewFactSheet.aspx?csid=109 (Accessed July 20, 2018)

(3) Tysnes, O.-B., Storstein, A. Epidemiology of Parkinson's disease. *J. Neural. Transm.* **2017**, *124*, 901-905.

(4) Parkinson, J. An essay on the shaking palsy. *London, Sherwood, Neely and Jones* **1817**,

(5) Bedard, P. J., Blanchet, P. J., Levesque, D., Soghomonian, J. J., Grondin, R., Morissette, M., Goulet, M., Calon, F., Falardeau, P., Gomez-Mancilla, B., Doucet, J. P., Robertson, G. S., Di Paolo, T. Pathophysiology of L-dopa-induced dyskinesias. *Mov. Dis.* **1999**, *14*, 4-8.

(6) Jenner, P. Molecular mechanisms of L-DOPA-induced dyskinesia. *Nature Rev. Neurosci.* **2008**, *9*, 665-677.

(7) Cenci, M. A., *Pathophysiology of L-DOPA-Induced Dyskinesia in Parkinson's Disease*, in *Dopamine Handbook*, S. Dunnett, A. Björklund, L. Iversen, and S. Iversen, Editors. 2009, Oxford University Press: New York. p. 434-444.

(8) Jenner, P. Preventing and controlling dyskinesia in Parkinson's disease-a view of current knowledge and future opportunities. *Movement Disorders* **2008**, *23*, S585-S598.

(9) Smith, Y., Villalba, R. Striatal and extrastriatal dopamine in the basal ganglia: an overview of its anatomical organization in normal and Parkinsonian brains. *Movement Disorders* **2008**, *23*, S534-S547.

(10) Calabresi, P., Picconi, B., Tozzi, A., Ghiglieri, V., Di Filippo, M. Direct and indirect pathways of basal ganglia: a critical reappraisal. *Nature Neurosci.* **2014**, *17*, 1022-1030.

(11) Obeso, J. A., Rodríguez-Oroz, M. C., Benitez-Temino, B., Blesa, F. J., Guridi, J., Marin, C., Rodriguez, M. Functional organization of the basal ganglia: therapeutic implications for Parkinson's disease. *Movement Disorders* **2008**, *23*, S548-S559.

(12) Marino, M. J., Hess, J. F., Liverton, N. Targeting the metabotropic glutamate receptor mGluR4 for the treatment of diseases of the central nervous system. *Curr. Top. Med. Chem.* **2005**, *5*, 885-895.

(13) Corti, C., Aldegheri, L., Somogyi, P., Ferraguti, F. Distribution and synaptic localisation of the metabotropic glutamate receptor 4 (mGluR4) in the rodent CNS. *Neuroscience* **2002**, *110*, 403-420.

(14) Battaglia, G., Busceti, C. L., Molinaro, G., Giagioni, F., Traficante, A., Nicoletti, F., Bruno, V. Pharmacological activation of mGluR4 metabotropic glutamate receptors reduces nigrostriatal degeneration in mice treated with 1-methyl-4-phenyl-1,2,3,6-tetrahydropyridine. *J. Neuroscience* **2006**, *26*, 7222-7229.

(15) Bruno, V., Battaglia, G., Copani, A., D'Onofrio, M., Di Iorio, P., De Blasi, A., Melchiorri, D., Flor, J. P., Nicoletti, F. Metabotropic glutamate receptor subtypes as targets for neuroprotective drugs. *J. Cereb. Blood Flow Metab.* **2001**, *21*, 1013-1033.

(16) Hacker, M. L., Tonascia, J., Turchan, M., Currie, A., Heusinkveld, L., Konrad, P. E., Davis, T. L., Neimat, J. S., Phibbs, F. T., Hedera, P., Wang, L., Shi, Y., Shade, D. M., Sternberg, A. L., Drye, L. T., Charles, D. Deep brain stimulation may reduce the relative risk of clinically important worsening in early stage Parkinson's disease. *Parkinsonism Relat. Disord.* **2015**, *21*, 1177-1183.

(17) Hacker, M., Charles, D., Finder, S. Deep brain stimulation in early stage Parkinson's disease may reduce the relative risk of symptom worsening. *Parkinsonism Relat. Disord.* **2016**, *22*, 112-113.

(18) Hacker, M. L., DeLong, M. R., Turchan, M., Heusinkveld, L. E., L., O. J., Molinari, A. L., Currie, A. D., Konrad, P. E., Davis, T. L., Phibbs, F. T., Hedera, P., Cannard, K. R., Drye, L. T., Sternberg, A. L., Shade, D. M., Tonascia, J., Charles, D. Effects of deep brain stimulation on rest tremor progression in early stage Parkinson disease. *Neurology* **2018**, DOI: 10.1212/WNL.0000000000005903.

(19) Valenti, O., Mannaioni, G., Seabrook, G. R., Conn, P. J., Marino, M. J. Group III metabotropic glutamate-receptor-mediated modulation of excitatory transmission in rodent substantia nigra pars compacta dopamine neurons. *J. Pharmacol. Exp. Ther.* **2005**, *313*, 1296-1304.

(20) Betts, M. J., O'Neil, M. J., Duty, S. Allosteric modulation of the group III $mGlu_4$ receptor provides functional neuroprotection in the 6-hydroxydopamine rat model of Parkinson's disease. *Br. J. Pharmacol.* **2012**, *166*, 2317-2330.

(21) Vernon, A. C., Palmer, S., Datla, K. P., Zbarsky, V., Croucher, M. J., Dexter, D. T. Neuroprotective effects of metabotropic glutamate receptor ligands in a 6-hydroxydopamine rodent model of Parkinson's disease. *Eur. J. Neurosci.* **2005**, *22*, 1799-1806.

(22) Vernon, A. C., Zbarsky, V., Datla, K. P., Dexter, D. T., Croucher, M. J. Selective activation of group III metabotropic glutamate reeptors by L-(+)-2-amino-4-phosphonobutyric acid protects the nigrostriatal system against 6-hydroxydopamine toxicity in vivo. *J. Pharmacol. Exp. Ther.* **2007**, *320*, 397-409.

(23) Austin, P. J., Betts, M. J., Broadstock, M., O'Neil, M. J., Mitchell, S. N., Duty, S. Symptomatic and neuroprotective effects following activation of nigral group III metabotropic glutamate receptors in rodent models of Parkinson's disease. *Br. J. Pharmacol.* **2010**, *160*, 1741-1753.

(24) Moyanova, S. G., Mastroiacovo, F., Kortenska, L. V., Mitreva, R. G., Fardone, E., Santolini, I., Sobrado, M., Battaglia, G., Bruno, V., Nicoletti, F., Ngomba, R. T. Protective role for type 4 metabotropic glutamate receptors against ischemic brain damage. *J. Cereb. Blood Flow Metab.* **2011**, *31*, 1107-1118.

(25) Ponnazhagan, R., Harms, A. S., Thome, A. D., Jurkuvenaite, A., Gogliotti, R., Niswender, C. M., Conn, P. J., Standaert, D. G. The metabotropic glutamate receptor 4 positive allosteric modulator ADX88178 inhibits inflammatory responses in primary microglia. *J. Neuroimmune Pharmacol.* **2016**, *11*, 231-237.

(26) Hampson, D. R., Rose, E. M., Antflick, J. E., *The Structures of Metabotropic Glutamate Receptor*, in *The Glutamate Receptors*, R.W. Gereau, IV and G.T. Swanson, Editors. 2008, Humana Press. p. 363-386.

(27) Conn, P. J., Pin, J.-P. Pharmacology and functions of metabotropic glutamate receptors. *Ann. Rev. Pharmacol. Toxicol.* **1997**, *37*, 205-237.

(28) Lindsley, C. W., Emmitte, K. A., Hopkins, C. R., Bridges, T. M., Gregory, K. J., Niswender, C. M., Conn, P. J. Practical strategies and concepts in GPCR allosteric modulator

discovery: recent advances with metabotropic glutamate receptors. *Chem. Rev.* **2016**, *116*, 6707-6741.

(29) Niswender, C. M., Conn, P. J. Metabotropic glutamate receptors: physiology, pharmacology, and disease. *Ann. Rev. Pharmacol. Toxicol.* **2012**, *50*, 295-322.

(30) Beurrier, C., Lopez, S., Révy, D., Selvam, C., Goudet, C., Lhérondel, M., Gubellini, P., Kerkerian-LeGoff, L., Acher, F., Pin, J.-P., Amalric, M. Electrophysiological and behavioral evidence that modulation of metabotropic glutamate receptor 4 with a new agonist reverses experimental parkinsonism. *FASEB J.* **2009**, *23*, 3619-3628.

(31) Selvam, C., Oueslati, N., Lemasson, I. A., Brabet, I., Rigault, D., Courtiol, T., Cesarini, S., Triballeau, N., Bertrand, H.-O., Goudet, C., Pin, J.-P., Acher, F. C. A virtual screening hit reveals new possibilities for developing group III metabotropic glutamate receptor agonists. *J. Med. Chem.* **2010**, *53*, 2797-2813.

(32) Selvam, C., Lemasson, I. A., Brabet, I., Oueslati, N., Karaman, B., Cabaye, A., Tora, A. S., Commare, B., Courtiol, T., Cesarini, S., McCort-Tranchepain, I., Rigault, D., Mony, L., Bessiron, T., McLean, H., Leroux, F. R., Colobert, F., Daniel, H., Goupil-Lamy, A., Bertrand, H.-O., Goudet, C., Pin, J.-P., Acher, F. C. Increased potency and selectivity for group III metabotropic glutamate receptor agonists binding at dual sites *J. Med. Chem.* **2018**, *61*, 1969-1989.

(33) Lindsley, C. W., Niswender, C. M., Engers, D. W., Hopkins, C. R. Recent progress in the development of mGluR4 positive allosteric modulators for the treatment of Parkinson's disease. *Curr. Top. Med. Chem.* **2009**, *9*, 949-963.

(34) Hopkins, C. R., Lindsley, C. W., Niswender, C. M. mGluR4-positive allosteric modulation as potential treatment for Parkinson's disease. *Future Med. Chem.* **2009**, *1*, 501-513.

(35) Robichaud, A. J., Engers, D. W., Lindsley, C. W., Hopkins, C. R. Recent progress on the identification of metabotropic glutamate 4 receptor ligands and their potential utility as CNS therapeutics. *ACS Chem. Neurosci.* **2011**, *2*, 433-449.

(36) Kalinichev, M., Le Poul, E., Bolea, C., Girard, F., Campo, B., Fonsi, M., Royer-Urios, I., Browne, S. E., Uslaner, J. M., Davis, M. J., Raber, J., Duvoisin, R., Bate, S. T., Reynolds, I. J., Poli, S., Celanire, S. Characterization of the novel positive allosteric modulator of the metabotropic glutamate receptor 4 ADX88178 in rodent models of neuropsychiatric disorders. *J. Pharmacol. Exp. Ther.* **2014**, *350*, 495-505.

(37) Bennouar, K.-E., Uberti, M. A., Melon, C., Bacolod, M. D., Jimenez, H. N., Cajina, M., Kierkerian-Le Goff, L., Doller, D., Gubellini, P. Synergy between L-DOPA and a novel positive allosteric modulator of metabotropic glutamate receptor 4: implications for Parkinson's disease treatment and dyskinesisa. *Neuropharmacol.* **2013**, *66*, 158-169.

(38) Engers, D. W., Niswender, C. M., Weaver, C. D., Jadhav, S., Menon, U. N., Zamorano, R., Conn, P. J., Lindsley, C. W., Hopkins, C. R. Synthesis and evaluation of a series of heterobiarylamides that are centrally penetrant metabotropic glutamate receptor 4 (mGluR4) positive allosteric modulators (PAMs). *J. Med. Chem.* **2009**, *52*, 4115-4118.

(39) Engers, D. W., Blobaum, A. L., Gogliotti, R. D., Cheung, Y.-Y., Salovich, J. M., Garcia-Barrantes, P. M., Daniels, J. S., Morrison, R. D., Jones, C. K., Soars, M. G., Zhuo, X., Hurley, J., Macor, J. E., Bronson, J. J., Conn, P. J., Lindsley, C. W., Niswender, C. M., Hopkins, C. R. Discovery, synthesis and pre-clinical characterization of *N*-(3-chloro-4-fluorophenyl)-1*H*-pyrazolo[4,3-*b*]pyridin-3-amine (VU0418506), a novel positive allosteric modulator of the metabotropic glutamate receptor 4 ($mGlu_4$). *ACS Chem. Neurosci.* **2016**, *7*, 1192-1200.

(40) Niswender, C. M., Jones, C. K., Lin, X., Bubser, M., Gray, A. T., Blobaum, A. L., Engers, D. W., Rodriguez, A. L., Loch, M. T., Daniels, J. S., Lindsley, C. W., Hopkins, C. R., Javitch, J. A., Conn, P. J. Development and antiparkinsonian activity of VU0418506, a selective positive allosteric modulator of metabotropic glutamate receptor 4 homomers without activity at mGlu2/4 heteromers. *ACS Chem. Neurosci.* **2016**, *7*, 1201-1211.

(41) https://parkinsonsnewstoday.com/2017/07/28/prexton-initiates-new-phase-2-trial-foliglurax-parkinsons-disease/ (Accessed July 20, 2018)

(42) Engers, D. W., Bollinger, S. R., Engers, J. L., Panarese, J. D., Breiner, M. M., Gregro, A., Blobaum, A. L., Bronson, J. J., Wu, Y.-J., Macor, J. E., Rodriguez, A. L., Zarmorano, R., Liang, S., Venable, D., Conn, P. J., Liindsley, C. W., Niswender, C. M., Hopkins, C. R. Discovery and characterization of N-(1,3-dialkyl-1H-indazol-6-yl)-1H-pyrazolo[4,3-b]pyridin-3-amine scaffold as mGlu4 positive allosteric modulators that mitigate CYP1A2 induction liability. *Bioorg. Med. Chem. Lett.* **2018**, 10.1016/j.bmcl.2018.1006.1034.

(43) Moss, T. A., Addie, M. S., Nowak, T., Waring, M. J. Room-temperature palladium-catalyzed coupling of heteroaryl amines with aryl or heteroaryl bromides. *Synlett* **2012**, *2*, 285-289.

(44) Bridges, T. M., Morrison, R. D., Byers, F. W., Luo, S., Daniels, J. S. Use of a novel rapid and resource-efficient cassette dosing approach to determine the pharmacokinetics and CNS distribution of small molecule 7-transmembrane receptor allosteric modulators in rat. *Pharmacol. Res. Perspect.* **2014**, *2*, e00077.

(45) Chen, C.-y., Andreani, T., Li, H. A divergent and selective synthesis of isomeric benzoxazoles from a single N-Cl imine. *Org. Lett.* **2011**, *13*, 6300-6303.

(46) Jones, C. K., Bubser, M., Thompson, A. D., Dickerson, J. W., Turle-Lorenzo, N., Amalric, M., Blobaum, A. L., Bridges, T. M., Morrison, R. D., Jadhav, S., Engers, D. W., Italiano, K., Bode, J., Daniels, J. S., Lindsley, C. W., Hopkins, C. R., Conn, P. J., Niswender, C. M. The mGlu4 positive allosteric modulator VU0364770 produces efficacy alone and in combination with L-DOPA or an adenosine A2A antagonist in preclinical rodent models of Parkinson's disease. *J. Pharmacol. Exp. Ther.* **2012**, *340*, 404-421.

(47) Fink, D. M., Strupczewski, J. T. Preparation of 6-fluorobenzisothazoles via a regioselective nucleophilic aromatic substitution reaction. *Tetrahedron Lett.* **1993**, *34*, 6525-6528.

(48) Clarke, K., Gleadhill, B., Scrowston, R. M. Condensed isothiazoles. Part 6. Compounds of potential biological interest obtained from 3-methyl-1,2-benzothiazole and its 5-substituted derivatives. *J. Chem. Res. (S)* **1979**, 395.

(49) https://www.eurofinsdiscoveryservices.com (Accessed July 20, 2018)

(50) Wouters, W., Janssen, C. G. M., Van Dun, J., Thijssen, J. B. A., Laduron, P. M. In vitro labeling of serotonin-S_2 receptors: synthesis and binding characteristics of [^{3}H]-7-aminoketanserin. *J. Med. Chem.* **1986**, *29*, 1663-1668.

Table of Contents graphic

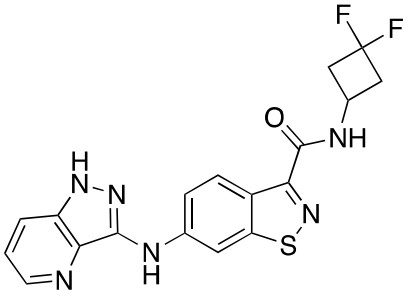

27o (VU6001376)
$hmGlu_4$ EC_{50} = 50 nM
$rmGlu_4$ EC_{50} = 45 nM
CL_p = 3.1 mL/min/kg
$t_{1/2}$ = 445 min
Active in haloperidol-induced catalepsy